2016-12

# An observational and analytical study of marginal ice zone atmospheric jets

Price, David M.

Monterey, California. Naval Postgraduate School


# NAVAL POSTGRADUATE SCHOOL

**MONTEREY, CALIFORNIA**

# THESIS

**AN OBSERVATIONAL AND ANALYTICAL STUDY OF MARGINAL ICE ZONE ATMOSPHERIC JETS**

by

David M. Price

December 2016

Thesis Advisor: Peter Guest
Second Reader: Wendell Nuss

THIS PAGE INTENTIONALLY LEFT BLANK

| REPORT DOCUMENTATION PAGE | | | *Form Approved OMB No. 0704–0188* |
|---|---|---|---|



| **1. AGENCY USE ONLY** *(Leave blank)* | **2. REPORT DATE** December 2016 | **3. REPORT TYPE AND DATES COVERED** Master's thesis |
|---|---|---|

| **4. TITLE AND SUBTITLE** AN OBSERVATIONAL AND ANALYTICAL STUDY OF MARGINAL ICE ZONE ATMOSPHERIC JETS | **5. FUNDING NUMBERS** |
|---|---|
| **6. AUTHOR(S)** David M. Price | |
| **7. PERFORMING ORGANIZATION NAME(S) AND ADDRESS(ES)** Naval Postgraduate School Monterey, CA 93943-5000 | **8. PERFORMING ORGANIZATION REPORT NUMBER** |
| **9. SPONSORING /MONITORING AGENCY NAME(S) AND ADDRESS(ES)** N/A | **10. SPONSORING / MONITORING AGENCY REPORT NUMBER** |

**11. SUPPLEMENTARY NOTES** The views expressed in this thesis are those of the author and do not reflect the official policy or position of the Department of Defense or the U.S. Government. IRB number ____N/A____.

| **12a. DISTRIBUTION / AVAILABILITY STATEMENT** Approved for public release. Distribution is unlimited. | **12b. DISTRIBUTION CODE** |
|---|---|

**13. ABSTRACT (maximum 200 words)**

Low-level atmospheric jets have been observed to occur frequently in marginal ice zones (MIZs), but little research has been done on the dynamics of these features. In the fall of 2015, during the Office of Naval Research "Sea State" cruise in the Beaufort Sea, the research team used radiosondes and shipboard instrumentation to detect several atmospheric jets in the atmospheric boundary layer or in the capping temperature inversion just above. The three strongest jets had maximum wind speeds at elevations near 350 m to 400 m elevation; one of these jets had a secondary maximum wind height at 900 m. Different theories have been suggested as reasons for the existence of MIZ jets, but in all the cases examined it appeared that the primary cause of the low-level jets was a thermal wind effect where the thermal wind opposes the geostrophic wind due to horizontal temperature changes in the atmospheric boundary layer and capping inversion. The jets were detected using rawinsonde measurements, complemented by daily runs of the ECMWF model. By comparing soundings that were perpendicular to the thermal gradients, it was possible to calculate how the geostrophic wind would vary with elevation. In most cases, the comparisons of the calculated thermal wind matched well with the observed winds in the upper part of the boundary layer, thus indicating that the low-level jets were primarily a result of a thermal wind opposing the background geostrophic wind. At the lowest levels, the observed winds speeds were less than the calculated geostrophic wind, as expected, due to friction.

| **14. SUBJECT TERMS** low level jet, Arctic, marginal ice zone | **15. NUMBER OF PAGES** 87 |
|---|---|
| | **16. PRICE CODE** |

| **17. SECURITY CLASSIFICATION OF REPORT** | **18. SECURITY CLASSIFICATION OF THIS PAGE** | **19. SECURITY CLASSIFICATION OF ABSTRACT** | **20. LIMITATION OF ABSTRACT** |
|---|---|---|---|
| Unclassified | Unclassified | Unclassified | UU |

NSN 7540–01-280-5500 Standard Form 298 (Rev. 2–89)
Prescribed by ANSI Std. 239–18

THIS PAGE INTENTIONALLY LEFT BLANK

**Approved for public release. Distribution is unlimited.**

# AN OBSERVATIONAL AND ANALYTICAL STUDY OF MARGINAL ICE ZONE ATMOSPHERIC JETS

David M. Price
Lieutenant, United States Navy
B.S., United States Naval Academy, 2011

Submitted in partial fulfillment of the
requirements for the degree of

**MASTER OF SCIENCE IN METEOROLOGY AND PHYSICAL OCEANOGRAPHY**

from the

**NAVAL POSTGRADUATE SCHOOL**
**December 2016**

Approved by: Peter Guest
Thesis Advisor

Wendell Nuss
Second Reader

Wendell Nuss
Chair, Department of Meteorology

THIS PAGE INTENTIONALLY LEFT BLANK

# ABSTRACT

Low-level atmospheric jets have been observed to occur frequently in marginal ice zones (MIZs), but little research has been done on the dynamics of these features. In the fall of 2015, during the Office of Naval Research "Sea State" cruise in the Beaufort Sea, the research team used radiosondes and shipboard instrumentation to detect several atmospheric jets in the atmospheric boundary layer or in the capping temperature inversion just above. The three strongest jets had maximum wind speeds at elevations near 350 m to 400 m elevation; one of these jets had a secondary maximum wind height at 900 m. Different theories have been suggested as reasons for the existence of MIZ jets, but in all the cases examined it appeared that the primary cause of the low-level jets was a thermal wind effect where the thermal wind opposes the geostrophic wind due to horizontal temperature changes in the atmospheric boundary layer and capping inversion. The jets were detected using rawinsonde measurements, complemented by daily runs of the ECMWF model. By comparing soundings that were perpendicular to the thermal gradients, it was possible to calculate how the geostrophic wind would vary with elevation. In most cases, the comparisons of the calculated thermal wind matched well with the observed winds in the upper part of the boundary layer, thus indicating that the low-level jets were primarily a result of a thermal wind opposing the background geostrophic wind. At the lowest levels, the observed winds speeds were less than the calculated geostrophic wind, as expected, due to friction.

THIS PAGE INTENTIONALLY LEFT BLANK

# TABLE OF CONTENTS

# LIST OF FIGURES

THIS PAGE INTENTIONALLY LEFT BLANK

# LIST OF ACRONYMS AND ABBREVIATIONS

| | |
|---|---|
| AGL | above ground level |
| AI | Arctic inversion |
| ABL | atmospheric boundary layer |
| COAMPS | Coupled Ocean/Atmosphere Mesoscale Prediction System |
| DRI | Directed Research Initiative |
| ECMWF | European Center for medium range weather forecasting |
| LLJ | low level jet |
| MIZ | marginal ice zone |
| MKS | Meters, Kilograms, Seconds |
| NIC | National Ice Center |
| NOAA | National Oceanic and Atmospheric Administration |
| NRL | Naval Research Laboratory |
| ONR | Office of Naval Research |
| USN | United States Navy |
| UTC | Coordinated Universal Time |
| YD | year day or day of year (Noon Jan 1 = YD 1.5) |

THIS PAGE INTENTIONALLY LEFT BLANK

# ACKNOWLEDGMENTS

This research was funded by the Office of Naval Research Arctic and Global Prediction Program via the Departmental Research Initiative “Sea State and Boundary Layer Physics of the Emerging Arctic Ocean,” Scott Harper and Martin Jeffries, program managers.

I would like to thank Professor Peter Guest for all of his help and guidance throughout this thesis. I would also like to thank my wife, Lindsay, and daughter, Kinsley, for their support throughout my entire time at the Naval Postgraduate School.

THIS PAGE INTENTIONALLY LEFT BLANK

# I. INTRODUCTION

## A. THESIS OBJECTIVES

Significant changes in the Arctic environment in recent years have renewed interest in studying the region by the scientific community. These changes in the Arctic include the types of atmospheric features that occur. This is especially true throughout the late summer and early winter months of September through November when sea ice cover and thickness has dramatically diminished from previous years. A feature that is becoming more common in the Arctic is low-level jets (LLJ). These events, although they only last for a few days, can have significant impacts on the local sea ice. During the jet event, the increased wind speed creates more waves in the arctic. These waves prevent flat ice sheets such as nilas from forming and instead cause the formation of pancake ice. Pancake ice appears to be much more prevalent in the Beaufort Sea region recently. The understanding of low-level jets is important not only for ice formation predictions but it will also impact future forecasting efforts in the marginal ice zone (MIZ) to include wave, sea ice, sea spray, and icing forecasts. This thesis will analyze the selected LLJs in the Arctic, with the goal of understanding the reason for the jet formations, their relation to the MIZ variations and synoptic scale meteorology, and their impact on the MIZ wave and ice physics.

## B. IMPORTANCE OF STUDY

Identifying the cause and generation mechanisms of these LLJs is a step toward understanding the changing Arctic environment as a whole. As the sea ice extent in the Arctic decreases, there is a potential for increased human activity. Increased activity could include but is not limited to military, commercial tourism, oil and gas development, fishing and even private endeavors (Navy 2014). By understanding these jets, the ability to forecast for these events and understand the impacts they can potentially have will help those that choose to operate in the Arctic do so in a safer manner.

## C. NAVAL APPLICATION

Just as in the scientific community, the changing Arctic has also attracted the attention of the United States Navy. As outlined in the Navy Arctic Roadmap, the U.S. Navy intends to increase the amount of surface operations conducted in the Arctic and these areas of pancake ice are potentially navigable areas (Navy 2014). As the Navy operates more frequently in the Arctic region understanding the emerging Arctic environment will not only be a necessity for safe operation, but also an advantage when required to respond to potential contingencies in the region (Navy 2014). U.S. Navy vessels were not designed with frequent Arctic operations in mind therefore it is critical that the Navy be able to predict and understand the impact of severe Arctic weather events, such as marginal ice zone jets, on their future operations in the Arctic region.

# II. LOW-LEVEL JETS

## A. LOW-LEVEL JETS IN THE ARCTIC

Low level jets are atmospheric phenomena that occur worldwide. The Arctic is no exception to this and some estimates place the rate of occurrence at between 25% and 50% of the time (Jakobson et al. 2013). For the purpose of this research, a LLJ was determined using the criteria set forth by Stull (1988), which define a jet as an area with winds $2ms^{-1}$ greater than the area immediately above it. These jets typically occur within the temperature inversion that exists near the surface. Formed as a result of longwave radiational cooling of the ice surface, the Arctic Inversion (AI) is a consistent occurrence in the arctic with the top usually located somewhere between 500 and 1500 m (Persson et al. 2016).Having identified the AI as the top of the potential jet region, the bottom is defined by the atmospheric boundary layer (ABL). This means that the jet will occur between the top of the ABL and the top of the AI, which is a range of about 600 to 800 m. It is worth noting that the LLJs typically occur right above the ABL (Figure 1.) Typical atmospheric profiles for the Arctic in both summer and winter are shown in (Figure 1). This study took place in the winter, which when compared to summer features the AI and ABL are slightly higher in altitude and thus the LLJ also takes place higher in the atmosphere. As we shall see in this thesis, LLJs can also extend into the ABL.

Figure 1. Arctic Temperature and Wind Speed Profiles. Source: Persson et al. (2016).

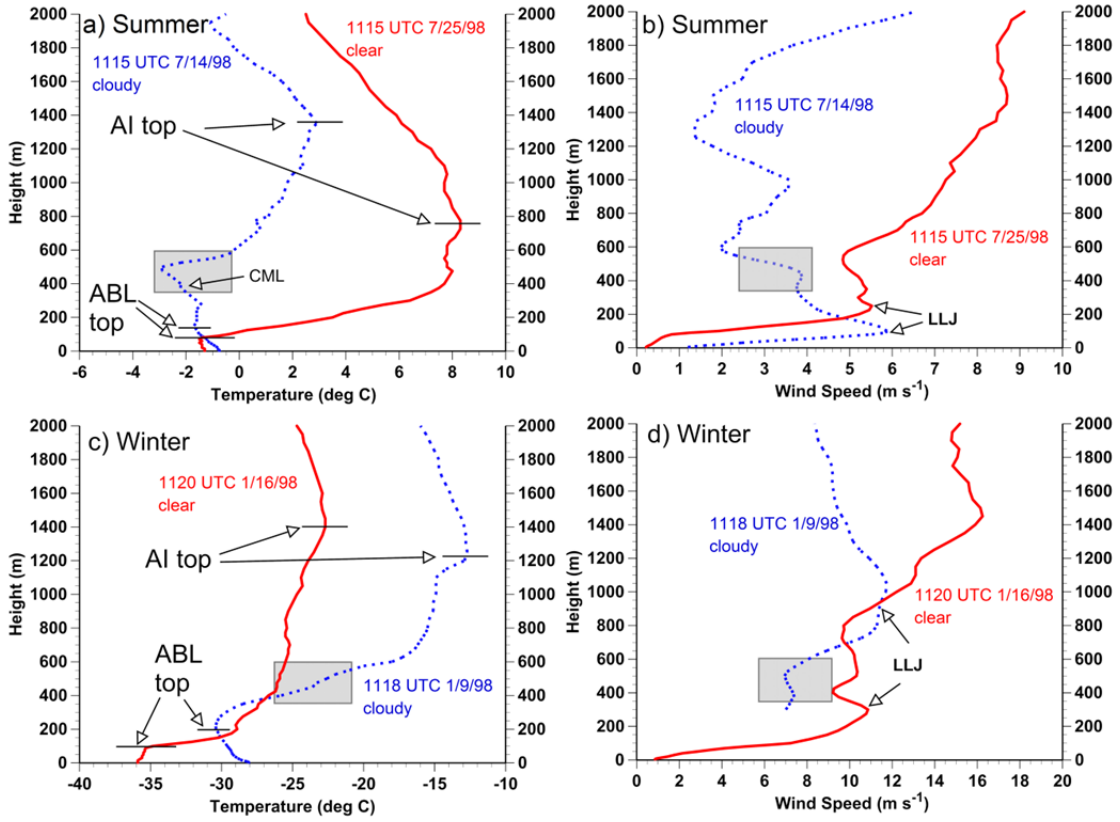


Image taken from Persson et al. (2016) shows the typical temperature and wind speed profiles for the Arctic broken out into summer and winter conditions.

## B. ARCTIC LLJ GENERATION PROCESSES

### 1. Inertial Oscillations

An early theory of how LLJs develop was the inertial oscillation hypothesis developed by Blackadar (1957). As summarized in Langland (1989), "A sudden reduction in mixed layer stress, which may occur at or after sunset, causes a temporary imbalance of forces in the boundary layer. The resultant ageostrophic wind component then undergoes an oscillation producing sub geostrophic and super geostrophic velocities." The oscillation of the event occurs when a stable stratified layer sets up and as the flow moves, the Coriolis force and the apparent centrifugal force are caused by the inertia of the fluid flow (Holton 2004) These oscillations are directly related to the inertial period of the region, which for the Arctic is about 12 hours (Persson et al. 2016).

This generation mechanism is similar to that of a nocturnal LLJ such as you might find in the United States Central plains (Holton 1966). In some literature, (Reiter 1961) a low level jet that is caused by an inertial oscillation is referred to as an inversion wind maxima. It is suggested in (Andreas et al. 2000) that LLJs formed by inertial oscillations occur over that ice pack, away from the MIZ.

## 2. Sea and Ice Breeze Circulations

Sea Breeze type circulations have been observed in the Arctic and are a potential generation mechanism of LLJs. It was discussed in (Kozo 1982) that sea breezes occur along the Alaskan Coast of the Beaufort Sea which is where some of the data were collected. Sea Breezes are the result of a horizontal temperature gradient setting up due to the differences in solar energy absorption by land and water. In the Arctic however, the sea breeze may actually have a significant alongshore component because of continuous solar irradiance, expanse of the coastline, and the large Coriolis force present (Moritz 1977). Due to orientation of the temperature gradient, common mid-latitude sea breezes occur perpendicular to the coast; however, the Coriolis force in the Arctic is significantly stronger. The Coriolis component means that in the Northern Hemisphere that this breeze would turn to the right. The alongshore component of these breezes could be perceived as a low-level jet.

An Ice breeze is similar to a sea breeze in that instead of it occurring at the land-sea interface, it occurs at the ice-sea interface. Instead of land being the relative heat source, in the case of an ice breeze, the water becomes the heat source meaning that an ice breeze has similar characteristics to the land breeze. Unlike baroclinically sourced LLJs, ice breezes blow toward low pressure and are therefore not geostrophic. The forcing mechanism on these jets is the same as a sea-land breeze, the differences in solar energy absorption and thus temperature of ice and water (Langland et al. 1989) which creates the low pressure area for the geostrophic wind to flow toward. The temperature difference above the two surfaces also allows for the establishment of a shallow front along the ice edge and it is at this front that the jet occurs. These types of breezes have been observed by both Revelle (2007) and Langland et al. (1989). In addition, during

(Langland et al. 1989) significant wind shear was observed in both the vertical and horizontal suggesting that baroclinicity also played a role in this LLJ formation. This lends to the theory that the LLJs studied during this research may have one or more of these generation processes contributing.

### 3. Other Potential Generation Processes

Gusts are considered to be a possible source of a perceived LLJ (Jakobson 2013). With the data collection that is available it is conceivable that a sounding would be impacted by a gust and would appear to have passed through a LLJ. This of course would not actually be a LLJ but rather a false positive in the data. This could be determined by decreasing the time between soundings since the time scale of a LLJ is much larger than that of a wind gust.

Traditionally, fronts are not actually a source of LLJs but rather credited with setting up conditions for LLJ generation (Jakobson 2013). Fronts could also potentially form a jet or like gusts, provide false positive data that would appear as a gust. Depending on data collection capabilities, the more frequent and expansive the data is the easier it would be to determine if an event is just a frontal passage and if the frontal passage set up conditions that eventually led to the formation of a LLJ. Regardless of whether the actual frontal passage appears as a gust or not it leaves behind favorable conditions for both baroclinically driven LLJs, and inertial oscillation LLJs.

### 4. Baroclinicity

Baroclinicity, when a temperature gradient is established along a constant pressure surface, can create LLJs. The LLJ from baroclinicity is the result of a temperature gradient that creates a thermal wind which can increase the wind speed in the area of the baroclinicity. Thus the horizontal temperature gradient causes a thermal wind which if oriented opposite the background geostrophic forcing creates a LLJ. It is noted in Jakobson (2013) that this type of LLJ is often associated with the passing of a transient cyclone through the area. When the cyclone is poleward of the ice edge, the resulting wind in the ice edge region can be parallel to the ice edge, with the ice to the right

looking downwind. This situation creates a thermal wind opposing the geostrophic wind, causing the wind speed to decrease with elevation, or in other words increasing toward the surface and hence creating the observed LLJs.

THIS PAGE INTENTIONALLY LEFT BLANK

# III. LOW-LEVEL JETS IN THE ARCTIC IN OCTOBER AND NOVEMBER 2015

## A. SEA STATE CRUISE

The data used in this project were collected during an Office of Naval Research (ONR) sponsored cruise from September 2015 through November 2015 on board the RV Sikuliaq in the Arctic Ocean. The cruise was the main experimental part of the Directed Research Initiative (DRI), "Sea State and Boundary Layer Physics of the Emerging Arctic Ocean" research initiative. During the cruise, four low-level jets (LLJ) were detected using radiosondes and surface measurements. Throughout the entire cruise the scientists were able to perform 169 radiosonde soundings. Of those 169 soundings, 83 of them took place during a low-level jet event or the immediate build up or dissipation of a jet.

## B. EQUIPMENT

All of the soundings from the cruise were taken using the Vaisala RS92-SGP Radiosonde. The radiosondes were attached to helium balloons and launched from the deck of the R/V Sikuliaq at varying intervals based on the capability of the scientists and synoptic conditions. The RS-92 contains sensors for Pressure, Temperature, and Humidity. The sensors are accurate to within 1 hPa for pressure, 0.5℃ for Temperature, and 5% Relative Humidity (Vaisala 2013). The radiosonde also contains a GPS unit to allow it to measure wind speed and direction. The GPS unit records position accurate to within 10 m horizontally and 20 m vertically (Vaisala 2013). The wind data from the GPS unit is accurate to within 0.15 m/s with directional uncertainty of 2 degrees (Vaisala 2013). Turbulent fluctuations could be much larger than these stated errors.

## C. YEAR DAY 285 EVENT

The first low-level jet occurred October 10–14, 2015 or year days 283 through 287. This LLJ and the others in the study are given their titles by the approximate date of maximum jet velocity during the event. For example, the YD 285 event's maximum wind speeds occur on YD 285. This event took place during the time of least ice extent for the

entire cruise. At this time, there was still significant water and MIZ separating the North Coast of Alaska from the solid ice pack. The soundings for this event were taken in the Beaufort Sea with the ship approximately 170 nautical miles northeast of Barrow, Alaska. The ship was operating in an area where the MIZ expanded up into the pack ice creating what resembled a bay. As depicted in Figure 2, the MIZ bay allowed the ship to travel farther to the north and have solid ice sheet to the east and west of its location. There were 31 soundings taken during this event, and Figure 3 gives a closer view of where each of these soundings was taken. The northern most sounding and southern most soundings were separated by 140 nautical miles. During the first day of the event YD 283, the ship was transiting east to west. From YD 284 until the conclusion of the event on YD 287 the ship was transiting on a Southwest – Northeast track with headings of about 315 degrees and 135 degrees. This means that the soundings collected were taken both across the direction of the jet (Easterly), though not parallel, and upwind and downwind in the jet.

Figure 2. Geographic Locations of Soundings during Year Day 285 Event


This google earth image shows the sounding locations and the ice edge from the National Ice Centers archived daily ice edge product. The land area to the south is Northern Alaska. The blue represents open ocean, the yellow represents areas of 1% to 79% ice coverage and the red represents areas of 80% to 100% ice coverage (National Ice Center, 2016).

Figure 3. Overview of the Soundings Taken during the YD 285 Event


The image shows a close up of when and where each sounding was taken. The sounding labels are in the format YYMMDDTT, with the times in UTC.

As the event began on October 10, the wind direction was approximately 090 degrees. As the event progressed the winds began to shift slightly to the East South East to approximately 100 degrees which was parallel to the ice edge. The event lasted nearly 96 hours which makes it the longest event that was analyzed and it produced the highest wind velocities. (Figure 4) shows a time series display of the event including wind speed and direction. The greatest intensity is focused around YD 285 with wind velocities remaining at or above 12 m/s through YD 287.

Figure 4. Time Height Plot of Event 285 Wind Speed and Direction

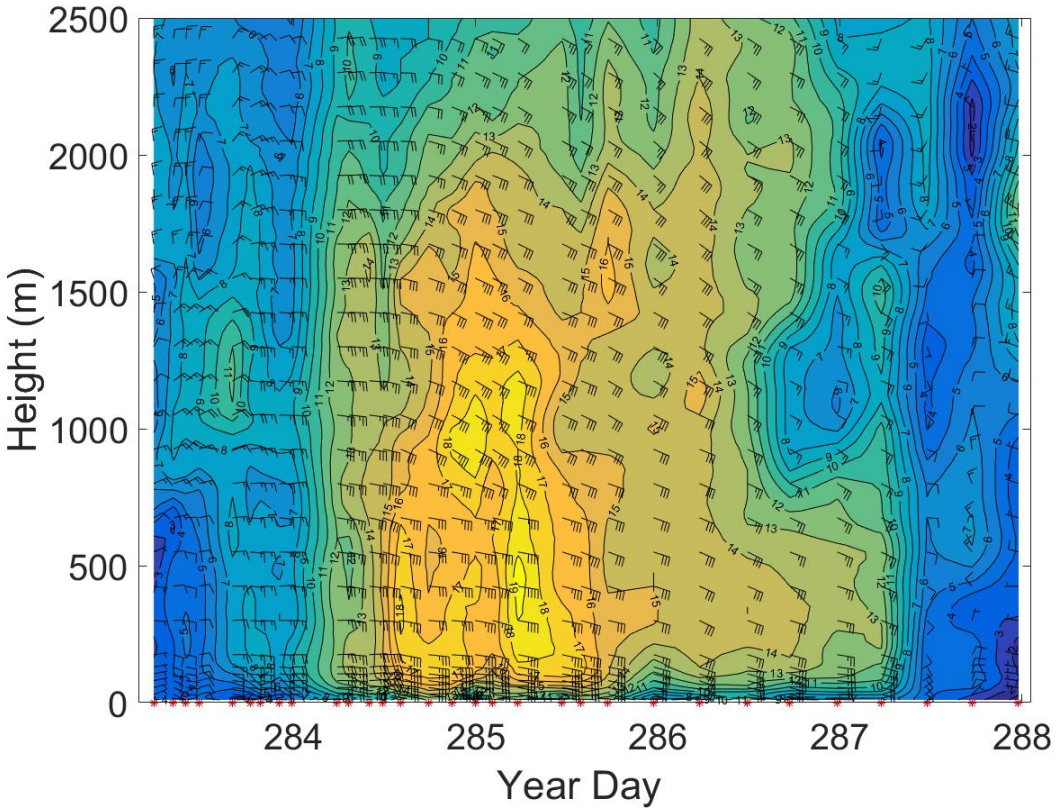


The time height plot of the Year Day 285 event shows the LLJ building through YD 285 where it reaches its maximum wind speed of 19m/s at a height of around 500 meters. From there the LLJ dissipates until YD 287 where it stops.

## D. YEAR DAY 292 EVENT

The second low-level jet occurred October 18–19, 2015 or year days 291 through 292. At the time of this event the ice extent had grown since the YD 285 event but there still remains both open water and MIZ separating the coast of Alaska from the solid ice pack. Unlike the YD 285 soundings that were taken in the Beaufort Sea these soundings were taken much further West in the Chukchi Sea which is shown in (Figure 5). The significance of the location is that soundings were not taken within the space between the North Coast of Alaska and the solid ice pack, and immediately to the south of there exists a large expanse of open ocean. Similar to the YD 285 event, the ship was in a bay created by the MIZ, though this feature was not nearly the size of the one experienced during the YD 285 event. The soundings of the event took place with the ship approximately 200

miles Northwest of Barrow, Alaska. There were only 13 soundings taken during this event due to its shorter duration. The locations of these soundings are shown in Figure 6. The southernmost soundings during the event were approximately 160 nautical miles Northwest of Barrow and the northernmost sounding were approximately 240 nautical miles Northwest of Barrow.

Figure 5. Geographic Locations of Soundings during Year Day 292 Event

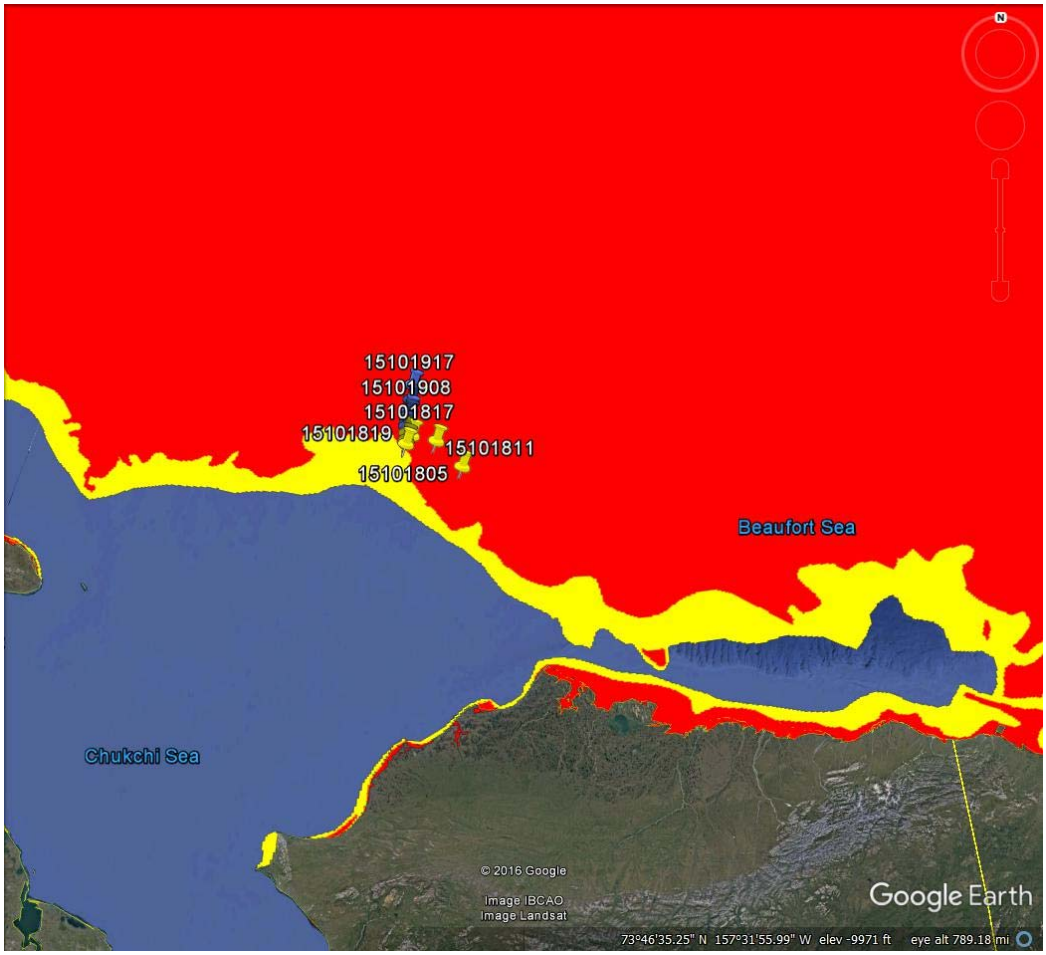


This google earth image shows the sounding locations and the ice edge as taken from the National Ice Centers archived daily ice edge product. The land area to the south is Northern Alaska, Barrow being near the northernmost part of Alaska. The blue shading represents open ocean, the yellow represents areas of 1% to 79% ice coverage, and the red represents areas of 80% to 100% ice coverage (National Ice Center, 2016).

Figure 6. Overview of the Soundings Taken during the YD 292 Event

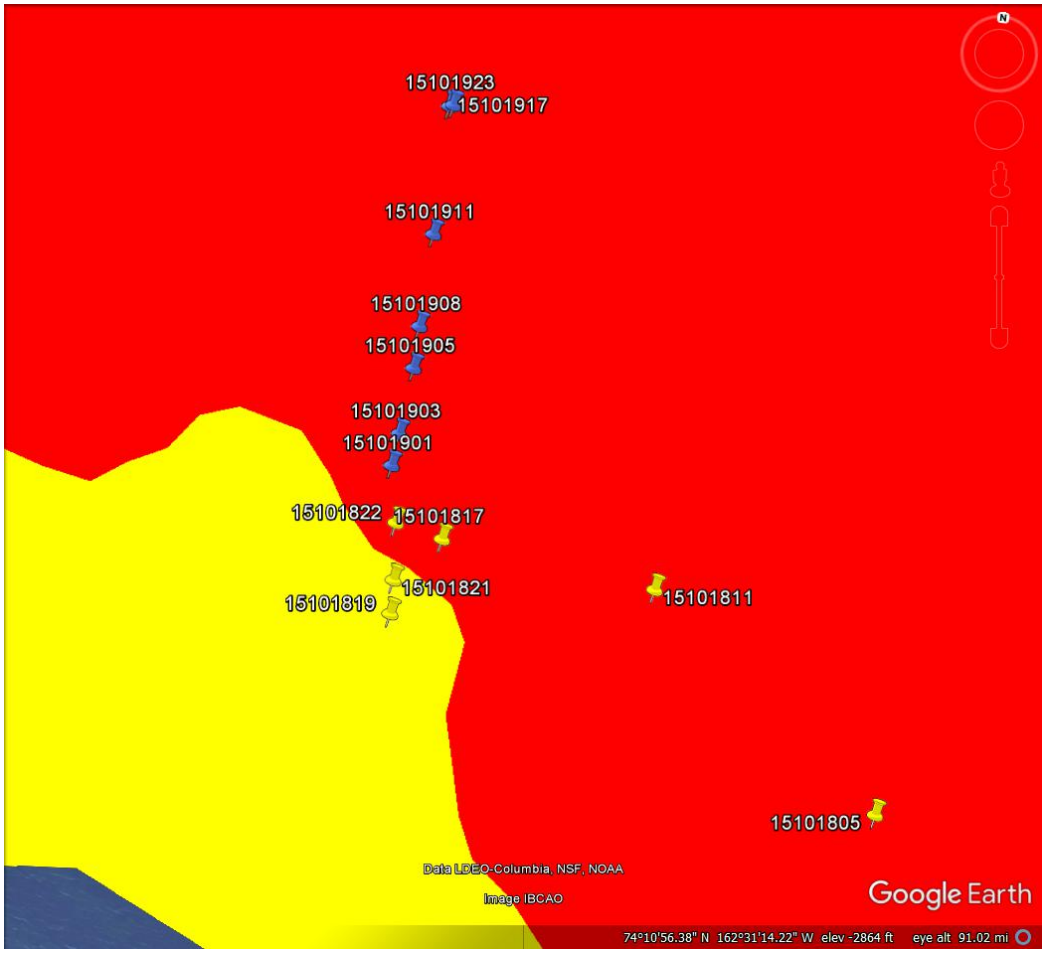


The image shows a close up of when and where each sounding was taken. The sounding labels are in the format YYMMDDTT, with the times in UTC.

As the event began on the 18th, the ship was transiting to the northwest and the soundings were performed while the winds were out of the east at approximately 080 degrees. Throughout YD 292 the LLJ intensified in velocity and shifted from easterly to northerly (near 000 degrees). Beginning with the 15101819 sounding, the ship begins to transit to the northeast and most directly into the jet.

This jet differed from the other jets in the study because of its lower intensity and the direction of the LLJ was perpendicular to the ice edge as opposed to parallel like the other cases analyzed. The horizontal time series of the wind speed and direction is shown in (Figure 7). Also, unlike the other events analyzed, this event lasts lasts for less than 24 hours.

Figure 7. Time Height Plot of Event 292 Wind Speed and Direction

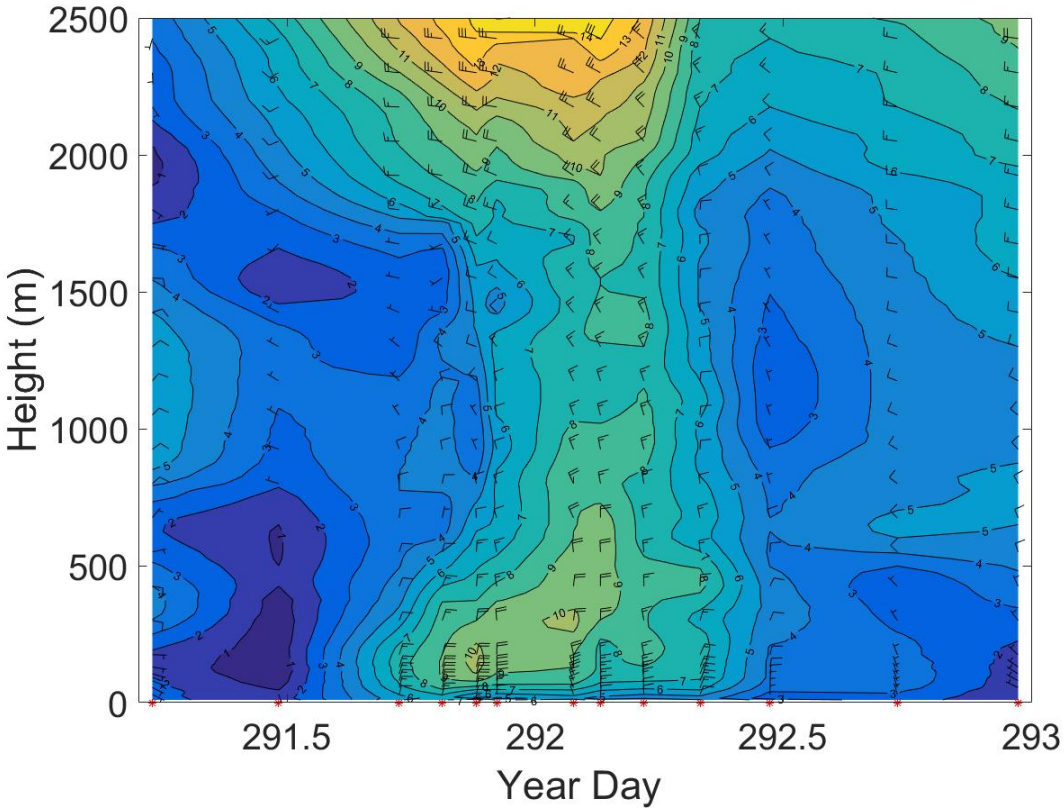


The time height plot of the Year Day 292 event shows the LLJ building through YD 292 where it reaches its maximum wind speed of 10m/s at a height of around 500 meters. Thereafter that, the LLJ dissipates and is completely gone by YD 292.5. Unlike the other case studies, this event has lower maximum wind speeds and a shorter time period during which it is active.

## E. YEAR DAY 297 EVENT

The next low-level jet occurred October 23–25, 2015 (year days 296 through 298). During this event the ice extent had again increased from YD 285 and YD 291 events. These sounding were collected in the Chukchi Sea with open ocean to the immediate south as shown in (Figure 8). The soundings of this event were taken as the ship operated approximately 100 Nautical miles North-North West of Barrow Alaska. There were 17 soundings taken during this event. The northern most sounding and southern most sounding were 85 nautical miles apart. The majority of the soundings were taken in a southwest to northeast alignment and while not exactly perpendicular to the LLJ direction the majority of the soundings are still across the axis of the LLJ which is

shown in (Figure 9). On the first day of the event, the ship transiting from north to south with several sounding taken at the same location (within 3nm) over several hours providing data about how the jet was changing temporally at a location. On the second day of the event, the ship transited southwest along an approximate heading of 220 and then reversed course and headed back northeast. On the third day of the event, soundings were taken at four locations that were not aligned.

Figure 8. Geographic Locations of Soundings during Year Day 297 Event

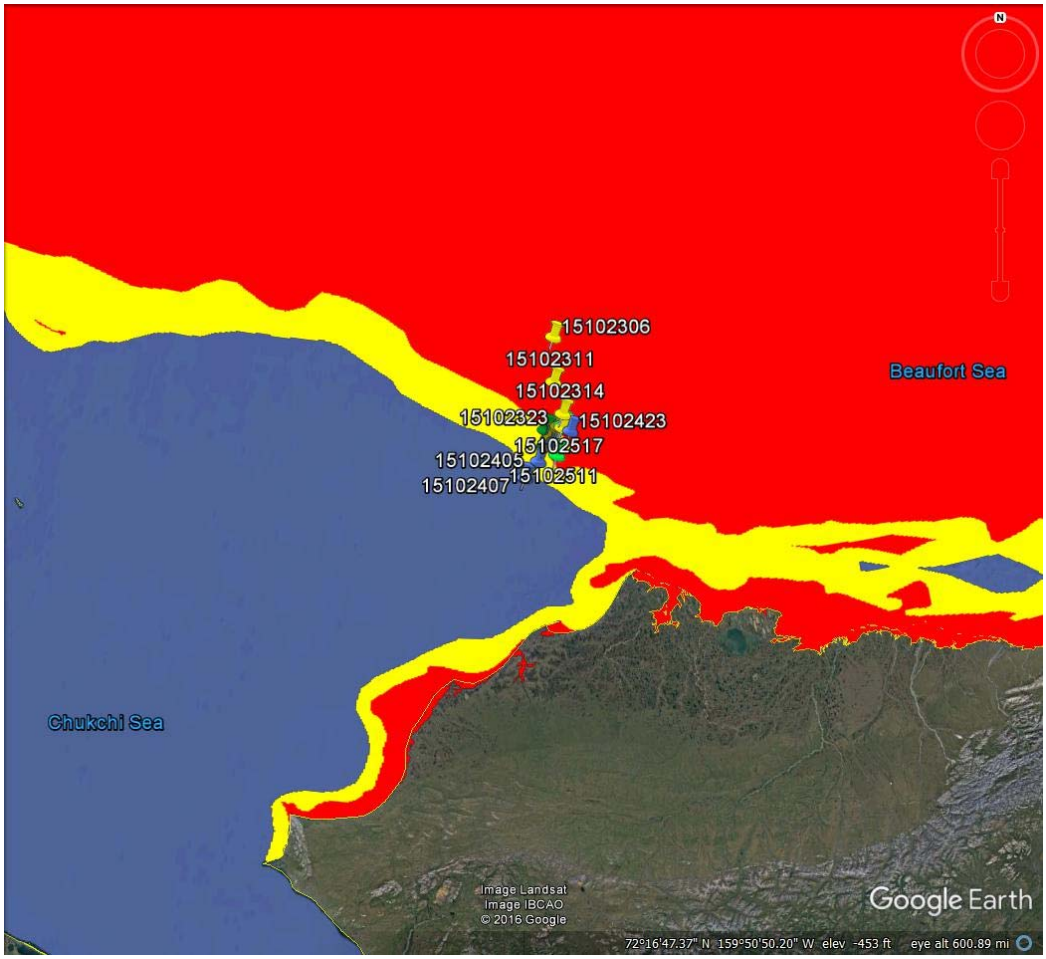


This google earth image shows the soundings and the ice edge as taken from the National Ice Centers archived daily ice edge product. The blue represents open ocean, the yellow represents areas of 1% to 79% ice coverage and the red represents areas of 80% to 100% ice coverage (National Ice Center, 2016).

Figure 9. Overview of the Soundings Taken during the YD 285 Event

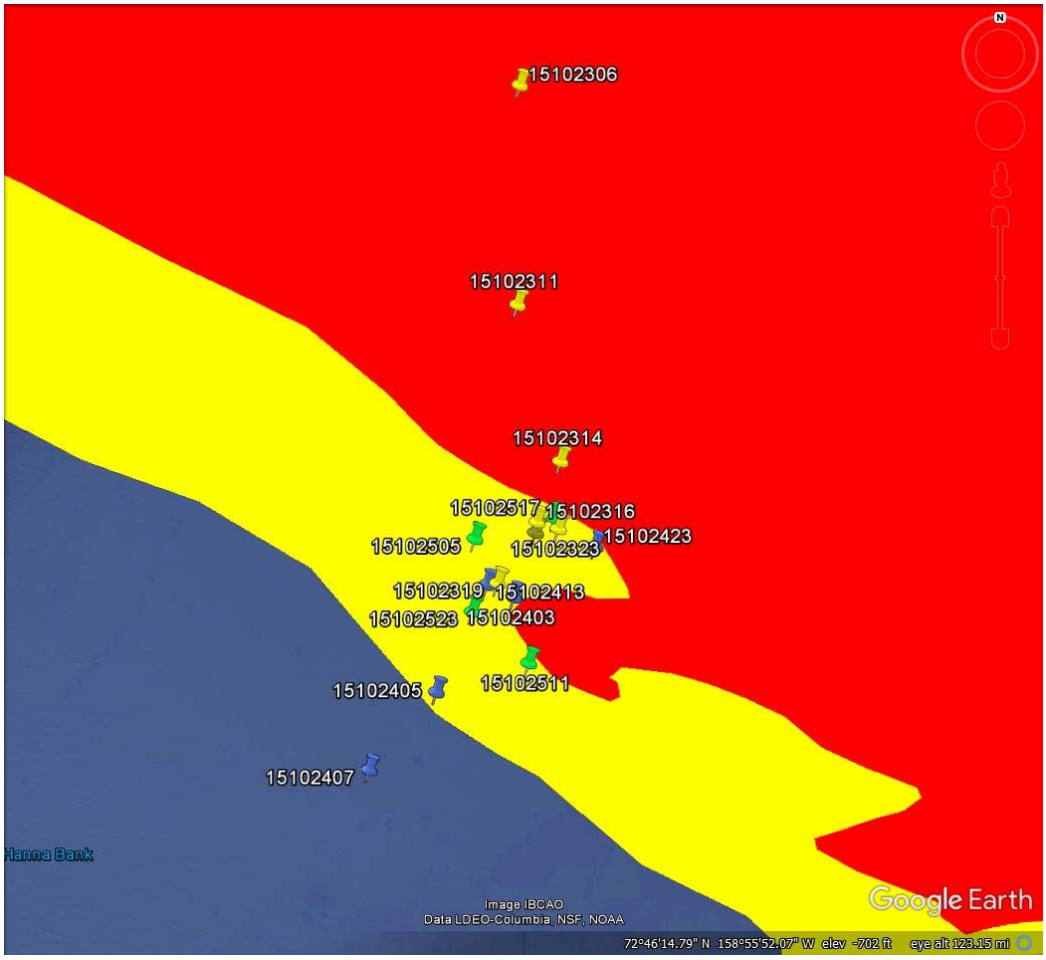


The image shows a close up of when and where each sounding was taken. The sounding labels are in the format YYMMDDTT, with the times in UTC.

The YD 297 event lasted about 36 hours making, it one of the shorter events analyzed. However, unlike the other short event on YD 291, this event had similar intensity to the other events with peak velocities nearing that of the YD 285 event. At the start of the event the wind direction was 090 degrees and as the event progresses the wind direction shifts to 100 degrees and then to 120 degrees which is shown in (Figure 10). These directions are generally parallel to the ice edge.

Figure 10. Time Height Plot of Event 297 Wind Speed and Direction

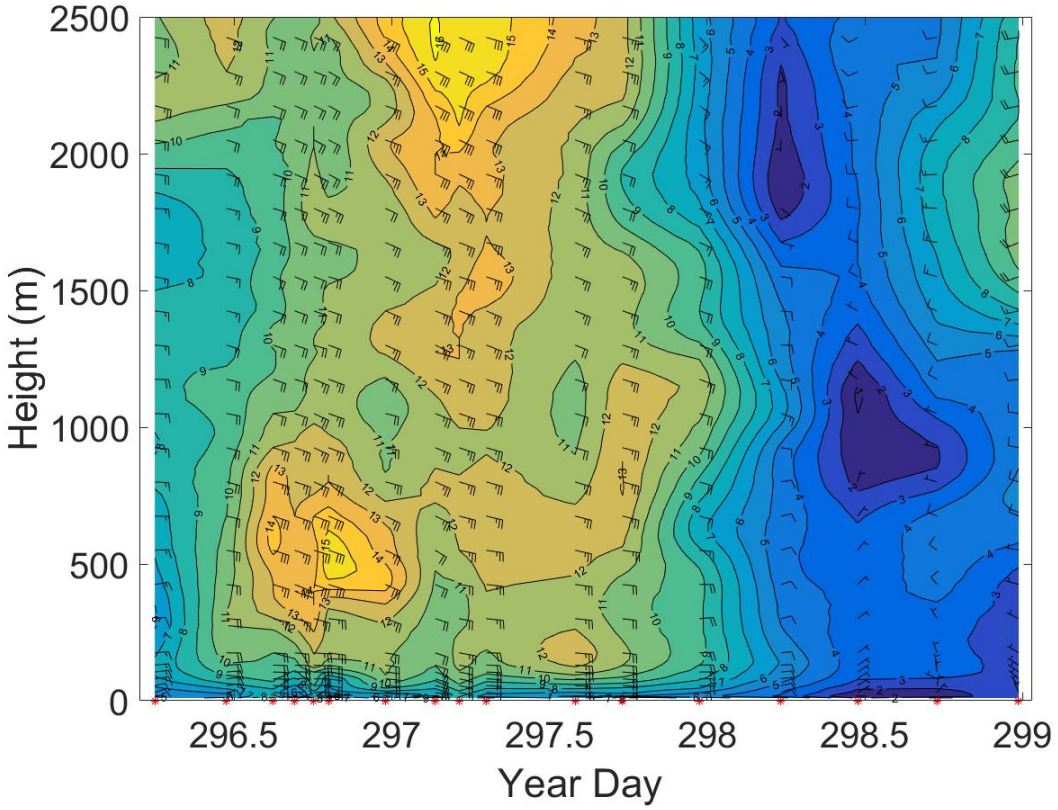


The time height plot of the Year Day 297 event shows the LLJ building through the end of YD 296 where it reaches its maximum wind speed of 15m/s at a height of around 500 meters. From there the LLJ dissipates until YD 298 where it stops.

## F. YEAR DAY 307 EVENT

The fourth and final observed low-level jet during the cruise took place November 1–5, 2015 which corresponds to year days 305 through 309. This event occurred during the greatest ice extent for the entire experiment. Unlike previous events that occurred while there was still open water or MIZ separating the Alaska coast from solid ice; this event occurred while there was solid ice all the way to the coast of Alaska. The soundings for this event were collected about 90 miles North West of Barrow, Alaska toward the beginning of the event and toward the end of the event they were collected as the ship began its transit out of the Arctic toward the Bering Strait (Figure 11). Due to the ship beginning its transit out of the area, the northern most sounding and southernmost

sounding are separated by 160 nautical miles. There were 22 soundings taken during this event which are shown in (Figure 12). The first three days of soundings are all taken with in the same 25 nautical mile circle. The last two days of soundings are aligned along the course 218 degrees during the ship transit mentioned before.

Figure 11. Geographic Locations of Soundings during Year Day 307 Event

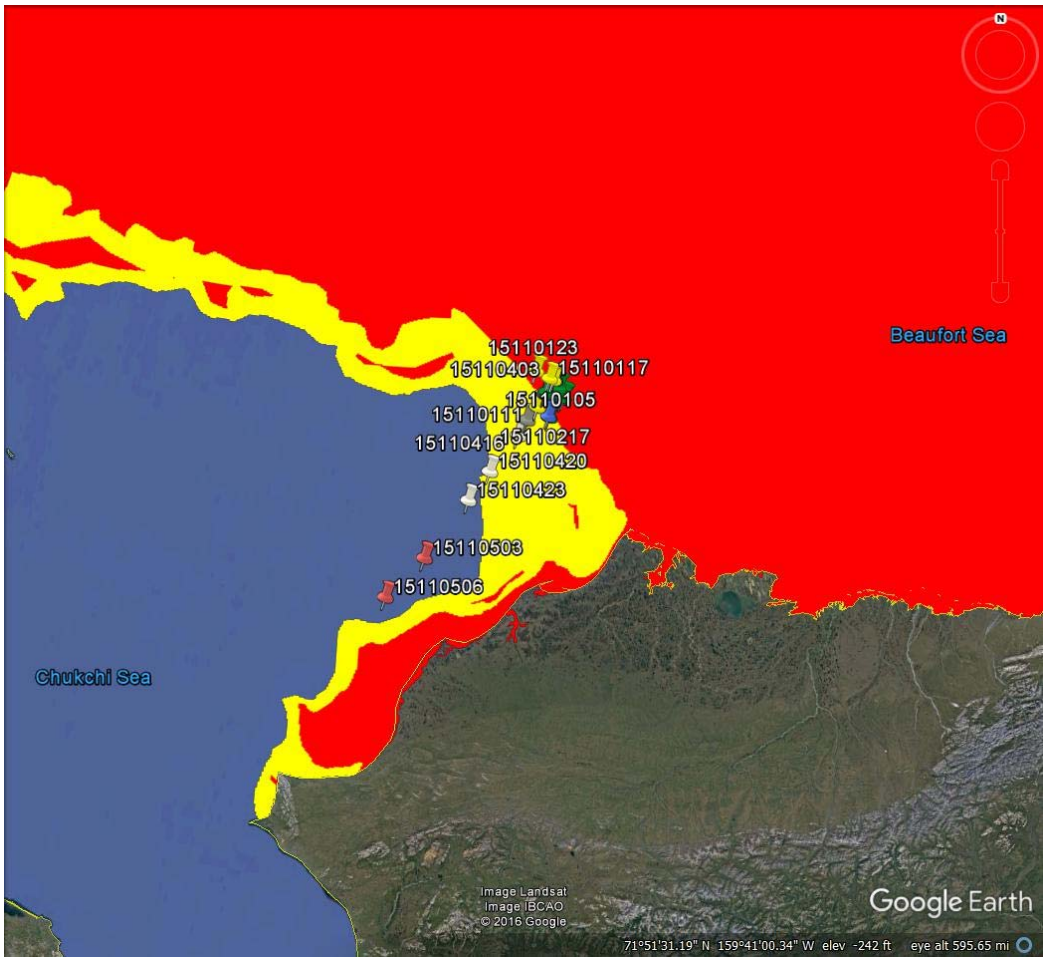


This google earth image shows the soundings and the ice edge as taken from the National Ice Centers archived daily ice edge product. The land mass in the Southeast corner of the map is northern Alaska. The blue represents open ocean, the yellow represents areas of 1% to 79% ice coverage and the red represents areas of 80% to 100% ice coverage (National Ice Center, 2016).

Figure 12. Overview of the Soundings Taken during the YD 307 Event

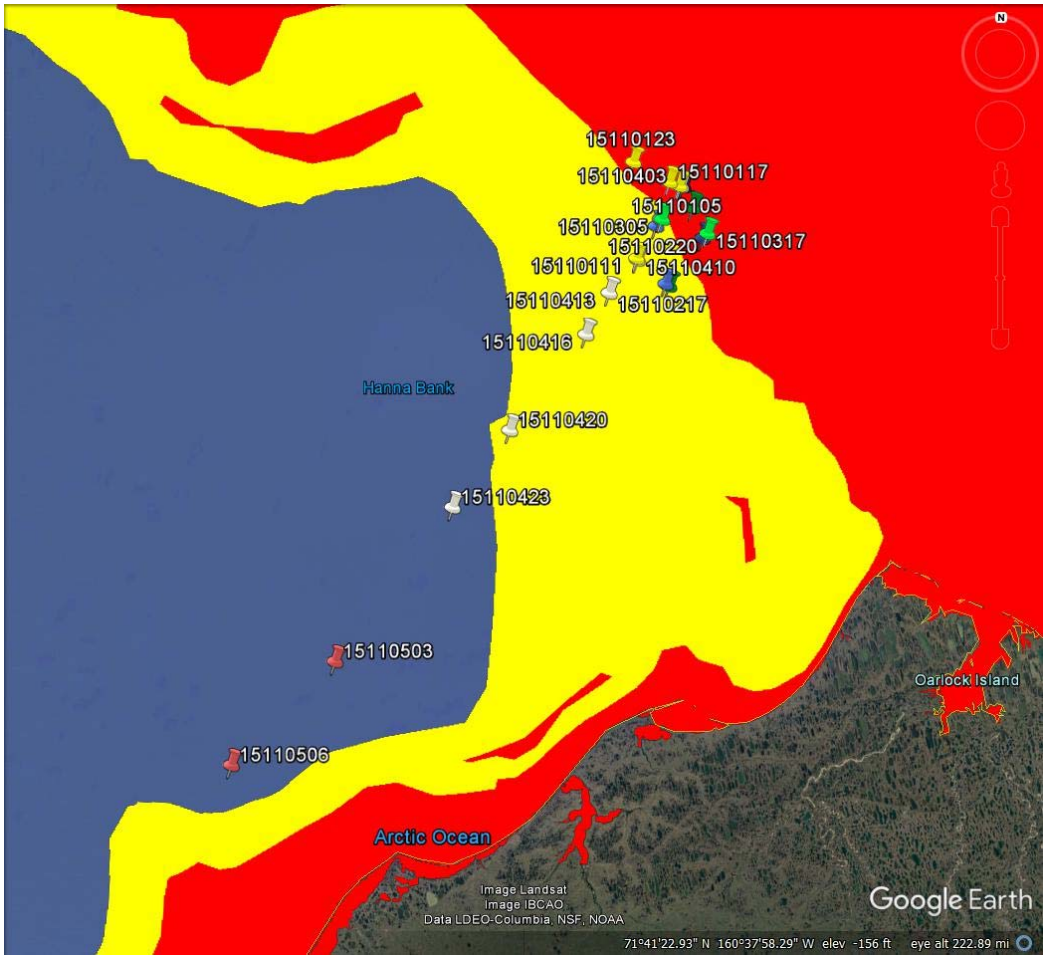


The image shows a close up of when and where each sounding was taken. The sounding labels are in the format YYMMDDTT, with the times in UTC.

The YD 307 event lasts nearly 72 hours and produced wind speeds that were similar to that of the YD 285 event. At the beginning of the event the winds were out of the East South East at around 120 degrees and they shifted to due East at 090 throughout the event which is shown in (Figure 13). While this represents a flow that is perpendicular to the ice edge at the location of the soundings, the ice edge is curved and the wind is flowing parallel to the ice edge immediately downstream.

Figure 13. Time Height Plot of Event 307 Wind Speed and Direction

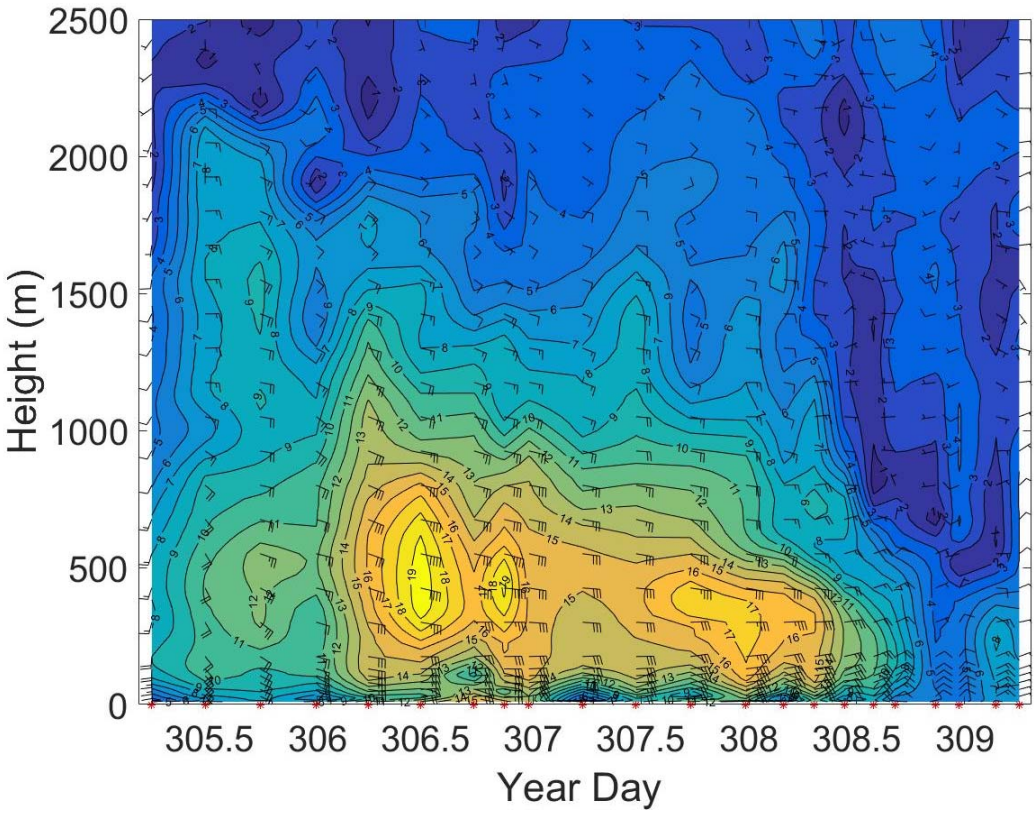


The time height plot of the Year Day 305 event shows the LLJ building through YD 306.5 where it reaches its maximum wind speed at a height of around 500 meters. From there the LLJ dissipates until YD 308.5 where it stops.

# IV. ANALYSIS OF LOW-LEVEL JETS IN THE ARCTIC

## A. METHODOLOGY

### 1. Data Challenges and Initial Analysis

When analyzing the data, several complexities were discovered that involved the movement of the ship while the data was being collected. First, because of the movement of the ship and the data being collected over time as opposed to all at once, the data set is changing both spatially and temporally throughout the experiment. Second, the ship direction and velocity were constantly changing so the data points do not have consistent spacing and are often not aligned in a constant direction. During the data analysis, an effort was made to identify data that were collected while the ship moved perpendicular to the direction of the jet and the time between data points was relatively small. That data is considered the "best" data for analysis and it was used more extensively to test hypotheses than other data.

The initial data set was plotted in time series form for wind speed, wind direction, and temperature in order to identify possible jets throughout the experiment. Upon initial analysis, four case studies were identified for further research. Once the LLJs to be analyzed were determined, the soundings were narrowed down to just the ones taken while the jet was active or during the immediate buildup and dissipation. This reduced the original set of 169 soundings to 83 that were applicable to the study.

### 2. Determining Spatial Relationships between Soundings

In order to address the temporal and spatial changes, the analysis was conducted using a combination of modern tools and more traditional methods. In order to gain an overview of how all of the data was collected, all of the sounding points for a particular event were plotted in Google Earth. Then the archived ice edge product for the corresponding day(s) were overlaid from the National Ice Center's (NIC) archived products website. This process resulted in an interactive map of all of the soundings for an event with the respective ice edge. The soundings are displayed simply by selecting a sounding on the display which allowed for the isolation of single soundings, days, or

periods throughout the event. This provided the ability to step through a jet event one sounding at a time and determine the space between the soundings, the bearing of transit between soundings, and the location of the sounding within the MIZ.

### 3. Temporal Analysis of the Soundings

To accurately couple the soundings with the spatial variation in their collection site, each sounding was analyzed first individually, and then as a set. The soundings were individually ingested into a MATLAB program which produced plots for temperature, wind speed, and wind direction. Once plots for all of the soundings in an event were generated, they were arranged in chronological order for each type of plot. The plots were then analyzed by overlaying one plot on the next plot in chronological order and using light shining through the plots to observe the changes. This was performed simultaneously for all of the variables considered, wind speed, temperature, and wind direction. Concurrently, the Google Earth map was used to identify the movement of the ship and the spatial relationship between the soundings. This allowed each sounding to be analyzed and to help determine if the changes in the environment were due to the change in location of the ship, the evolving event over time, or a combination of the two.

### 4. Quantitative Analysis

In order to produce a more quantitative result as to the characteristics of the geostrophic flow, the thermal wind equation was used. In all cases, a significant temperature gradient was present across the MIZ. The thermal wind equations can be expressed as follows (Stull 2009):

$$\partial U_g/\partial z = - (g/fT)(\partial T/\partial y)$$

$$\partial V_g/\partial z = + (g/fT)(\partial T/\partial x)$$

In order to eliminate the need to account for density differences that would have been necessitated by the thermal wind equations expressed in z coordinates, the equations were rewritten to be expressed in pressure coordinates. Once placed in component form the thermal wind equations become:

$$\partial u_g/\partial P = (R/fP)(\partial T/\partial y)_p$$

$$\partial v_g/\partial P = -(R/fP)(\partial T/\partial x)_p$$

For this thesis, standard meters, kilograms, seconds (MKS) units were used. The u and v components represent the x (north) and y (east) components of the geostrophic winds. T is the Virtual Temperature (K), P is the atmospheric pressure in $Kgs^{-2}m^{-1}$, R is the gas constant for dry air (287 J $Kg^{-1}$ $K^{-1}$), f is the Coriolis Parameter ($s^{-1}$) = $(2)(7.29x10^{-5})\sin(\text{latitude})$ which for the latitude in the study is about 1.39 x $10^{-4}$ ($s^{-1}$) (Holton 2004). The sub script p denotes that the value is along a constant pressure surface.

At this point in the analysis, some assumptions were made. First assumption was that the wind direction is constant with elevation. For most of the soundings, this is accurate within a range of about 10 degrees. The second assumption is that the wind direction is perpendicular to the pressure gradient which had to be checked at each sounding tested for validity. By making these assumptions the thermal wind equations were reduced from a pair of equations to just a single equation

$$\partial u/\partial P = (R/fP)(\partial T/\partial n)_p,$$

where now u is defined as the total geostrophic wind speed and n (natural coordinates) is the crosswind direction. By using the finite difference method in order to approximate a solution to the differential equation the resulting form is

$$\Delta u/\Delta P = (R/fP)(\Delta T/\Delta n)_p,$$

and by solving for the change in geostrophic wind speed the result is

$$\Delta u = \Delta P\ (R/fP_a)(\Delta T/\Delta n)_p$$

where $P_a$ is the average pressure throughout the entire change in pressure ($\Delta P$). The horizontal distance between soundings is represented by $\Delta n$ meters. At this point an assumption was made that the distance between soundings ($\Delta n$) was constant with elevation. In reality, there is some change in separation distance at different heights due

to balloon motion but this change is significantly smaller than the distance between soundings and is thus negligible. This means that the balloon was assumed to be at the surface location for the elevations where the LLJs occurred. If the entire sounding was being analyzed, this assumption would be inaccurate because the winds could carry the balloon 10s of kilometers downstream and the distance it traveled has the potential to be different than the distance between soundings. For our analysis only the bottom 2500 meters of the sounding are analyzed, so therefore we can make the constant separation distance assumption. Another assumption was that the virtual temperature gradients (which is really what thermal wind uses), are the same as the actual temperature gradients, a reasonable assumption given the relatively low values of specific humidity in the cold air.

The data from the sounding pairs needed to be normalized to the same pressure levels to apply the thermal wind equation. While the equations are written in MKS units, the pressure values can be expressed in hPa because they are used as a ratio. Similarly, the temperature units should be in Kelvin; however, since only the temperature difference is being used, they can remain in Celsius. Since Kelvin and Celsius are the same scale, with the only difference being the location of zero, the units will remain in Celsius as recorded in the sounding, thus simplifying the data analysis. There did need to be a one to one pressure level correspondence between data points for each sounding. In order to achieve this ratio, a constant pressure interval of 0.5 hPa was used. Values of pressure, temperature, and specific humidity were assigned to each 0.5 hPa interval by linearly interpolating from the two adjacent measured pressure levels. A pressure difference of 0.5 hPa between intervals represents 4 to 6 meters in the vertical, which is sufficiently fine without making the calculation overly burdensome.

The equations were then coded into MATLAB and designed to accept the sounding data from the cruise. The results, which are included in the results chapter, were generated in graphical form that showed the measured LLJ profile compared to the jet profile calculated by the thermal wind equations.

## B. INITIAL ANALYSIS

The initial analysis of the data involved plotting time series plots from the entire cruise in order to identify possible events for further study. Plotting wind speed over time was the best way to visually display possible jet events. In (Figure 14) the orange colored sections correspond to times of higher wind speed. The four events introduced earlier are clearly visible and they all show different characteristics of duration, max height, and intensity. A clearer depiction of the wind direction over time is shown in (Figure 15) with the orange and brown colors representing easterly winds that were consistent with the LLJ occurrences.

Figure 14. Time Height Plot of Wind Speeds and Direction for the Entire Cruise

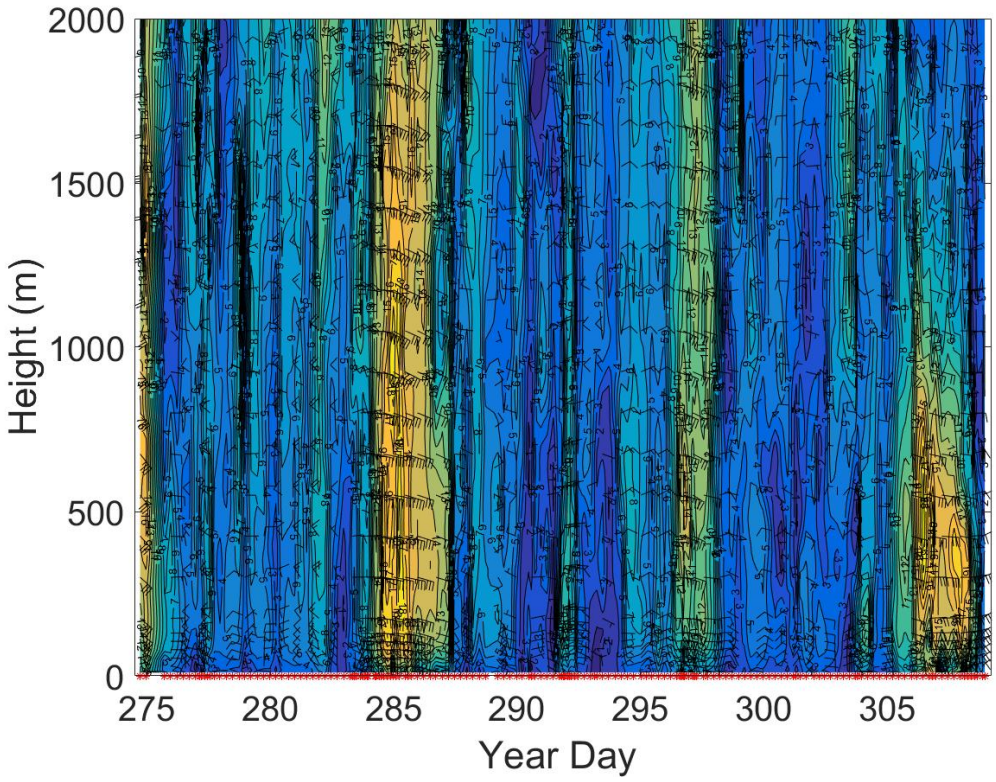


The time height plot of the wind speeds and direction for the entire cruise shows several distinct high wind events (orange-yellow colored fill).

Figure 15. Time Height Plot of Wind Direction for the Entire Cruise

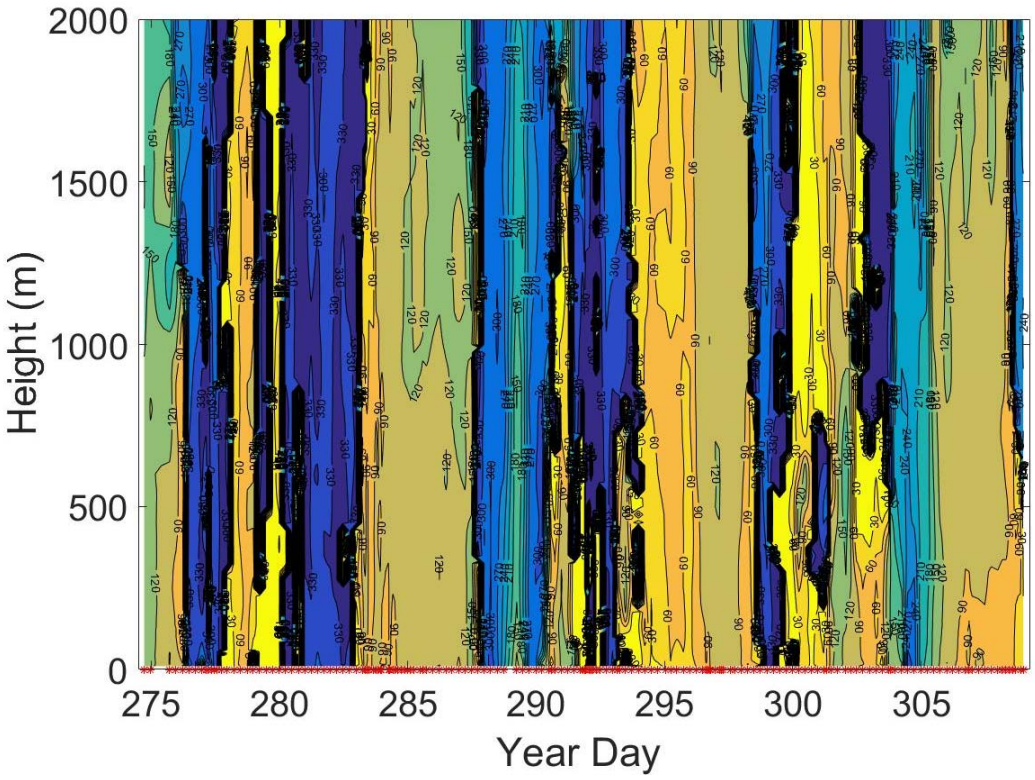


The time height plot of wind direction for the entire cruise shows the wind direction predominantly out of the East and the times that the wind is moving in this direction correlate to when the LLJs are active.

## C. YEAR DAY 285 EVENT

### 1. Synoptic Situation

The synoptic analysis was done using research data and archival weather prediction and depictions. For the purposes of visual characterization, the European Center for Medium Range Weather Forecasting (ECMWF) model was used. Whenever possible the zero hour step of the model was used but in some cases the 24 and 72 hour steps were needed because of gaps in the archived data.

During the first day of the analysis period (YD 283) for the YD 285 event the surface winds were predominantly out of the East. There was an area of higher winds to the southwest of the research vessels location (Figure 16). At the research location the model showed 9 m/s wind speed, which was consistent with the wind speed values measured during soundings from the same time period.

Figure 16. ECMWF Model Forecast valid October 10, 2015 at 1200 UTC

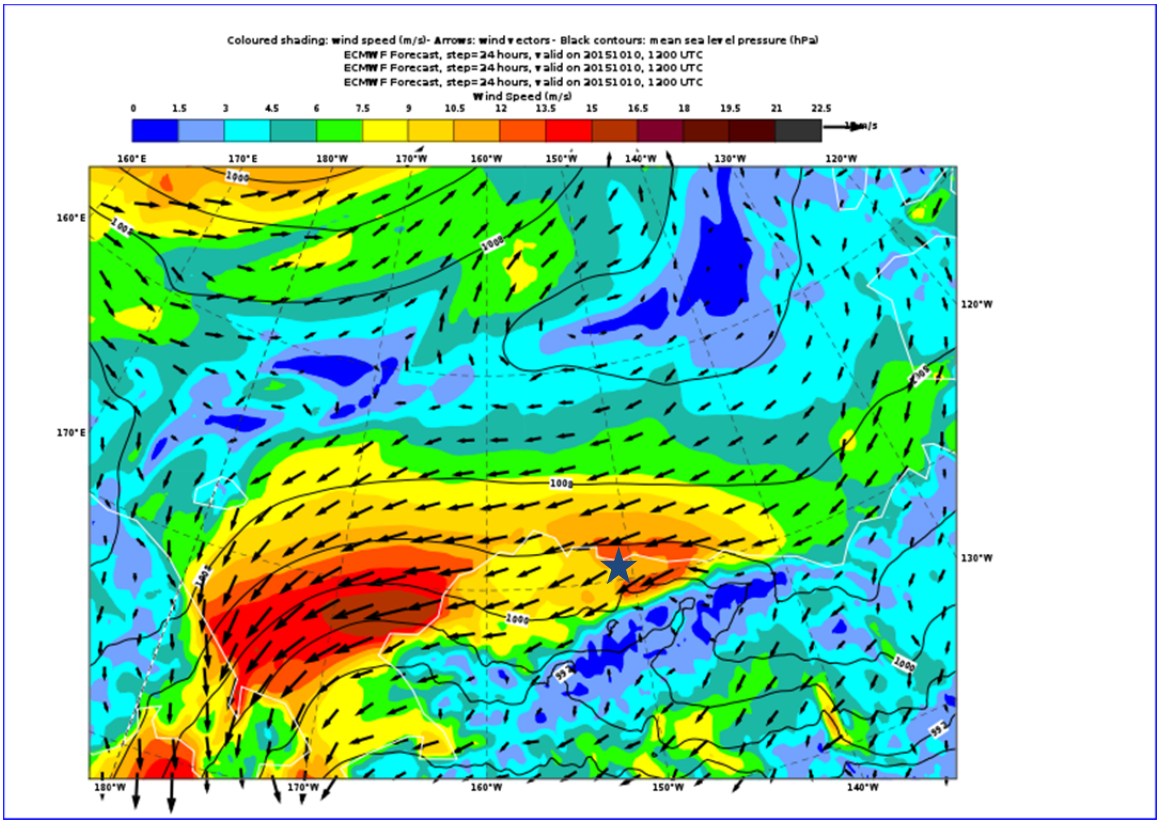


ECMWF forecast valid for 20151010 at 1200 UTC which was YD283, the first day of the YD285 event. This forecast was a 24 hour step from the initial model run. The ship location is denoted by the blue star. Winds are the 10m winds.

During the second day of analysis (YD 284), the surface winds in the region where the research vessel was located began to increase and were around 12 m/s, which was again consistent with the sounding data (Figure 17). The wind direction was also still easterly in the research area which is consistent with both the soundings and also parallel with the ice edge. Another important observation is that the winds are flowing parallel to the isobars meaning the wind was geostrophic.

Figure 17. ECMWF Model Forecast valid October 11, 2015 at 1200 UTC

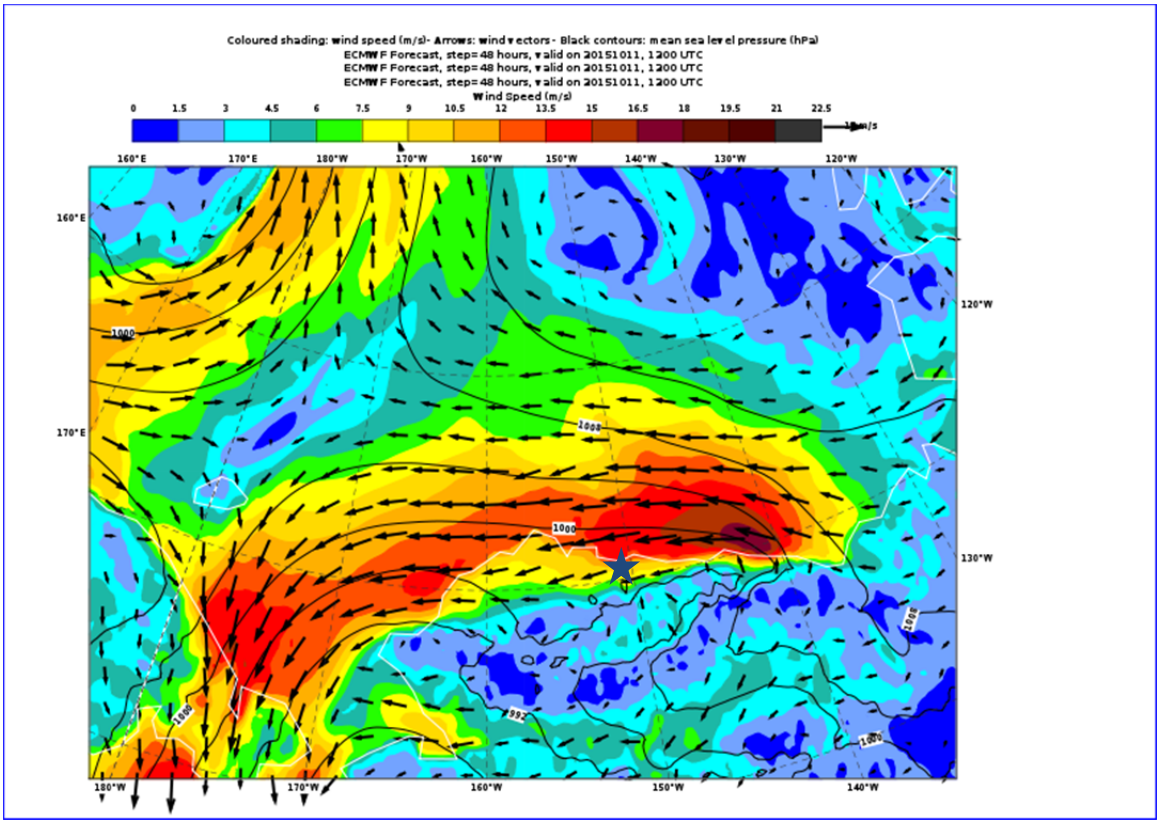


ECMWF forecast valid for 20151011 at 1200 UTC which was YD284, the second day of the YD285 event. This forecast was a 48 hour step from the initial model run. The ship location is denoted by the blue star. Winds are the 10m winds.

The third day of the analysis period (YD 285) had the greatest winds, according to the sounding data. The ECMWF model for this day was not available in the archive and thus (Figure 18) is the 72 hour step model from the first day of the analysis period. According to the soundings, the ECMWF shows the jet weakening a little prematurely. Nonetheless, the low pressure system that will eventually end the jet was visible to the northwest of the research area and was beginning to alter the pressure surface.

Figure 18. ECMWF Model Forecast valid October 12, 2015 at 1200 UTC

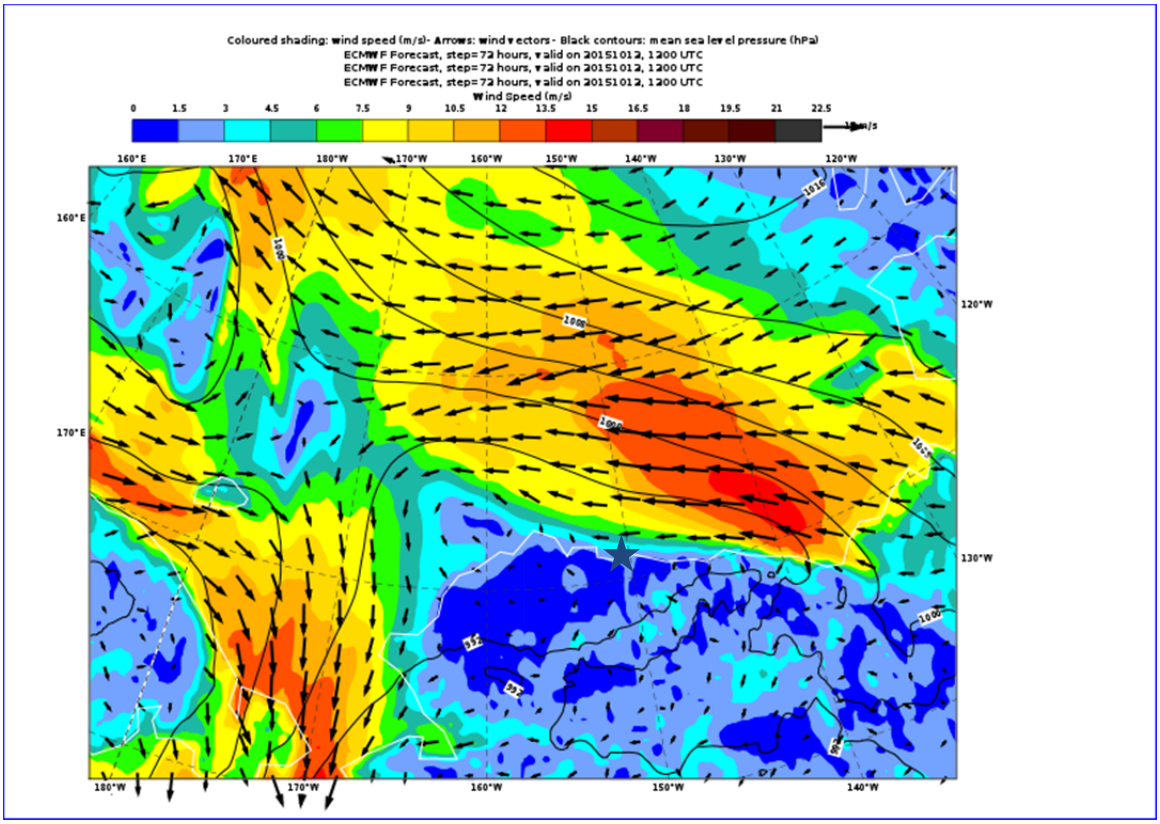


ECMWF forecast valid for 20151012 at 1200 UTC which was YD285, the third day of the YD285 event. This was the day with the strongest observed winds. This forecast was a 72 hour step from the initial model run. The ship location is denoted by the blue star. Winds are the 10m winds.

During the fourth day of the analysis period (YD 286) the jet began to weaken. This was the result of a low pressure system moving into the area (Figure 19). The low pressure system, which was to the northwest of the research area, caused the pressure surface to change and thus the pressure gradient and the temperature gradient were no longer aligned, which caused the jet to die out.

Figure 19. ECMWF Model Forecast valid October 13, 2015 at 1200 UTC

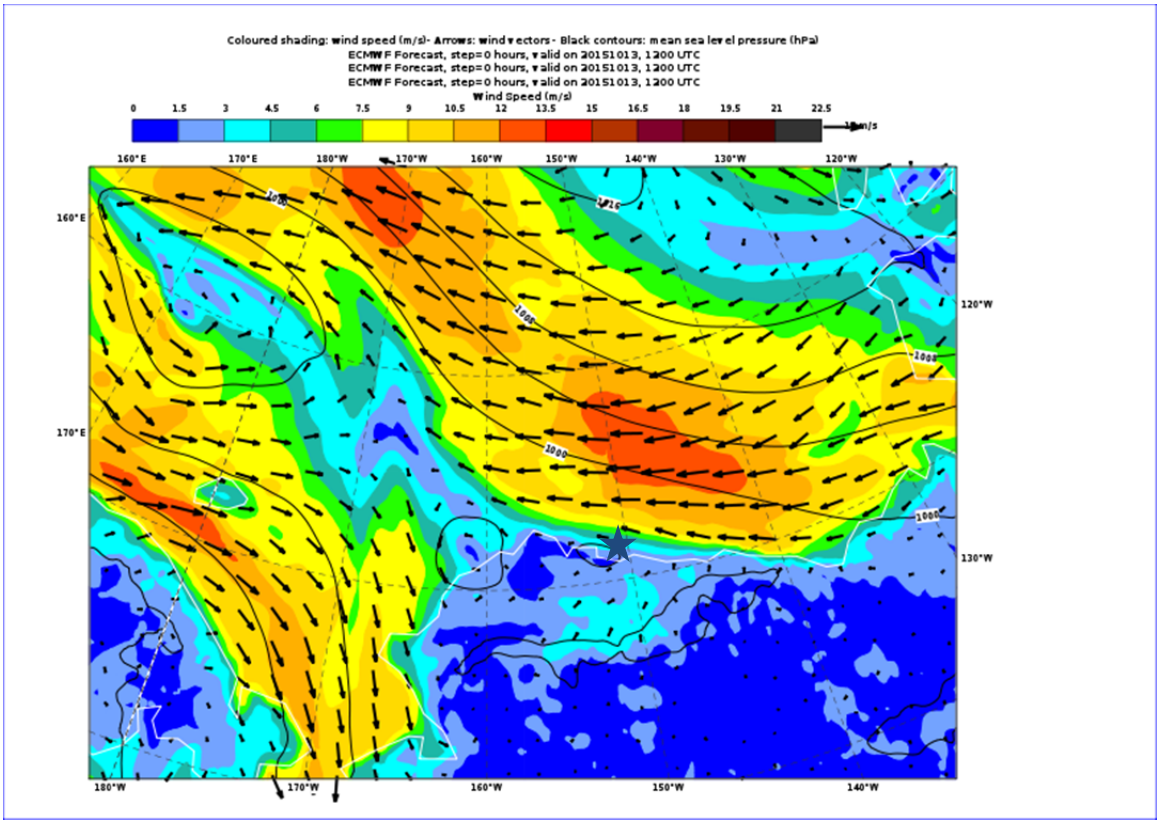


ECMWF forecast valid for 20151013 at 1200 UTC which was YD286, the fourth day of the YD285 event. This forecast was a 0 hour step from the initial model run. The ship location is denoted by the blue star. Winds are the 10m winds.

During the final day of the analysis period (YD 287) the low pressure system moved into the research area and broke up the LLJ. The low, shown in (Figure 20) was centered over the area that the soundings were being taken. The presence of the low was also evident in the soundings which recorded a decrease in wind speed and a distinct shift in the wind direction showing the influence of the low pressure system.

Figure 20. ECMWF Model Forecast valid October 14, 2015 at 1200 UTC

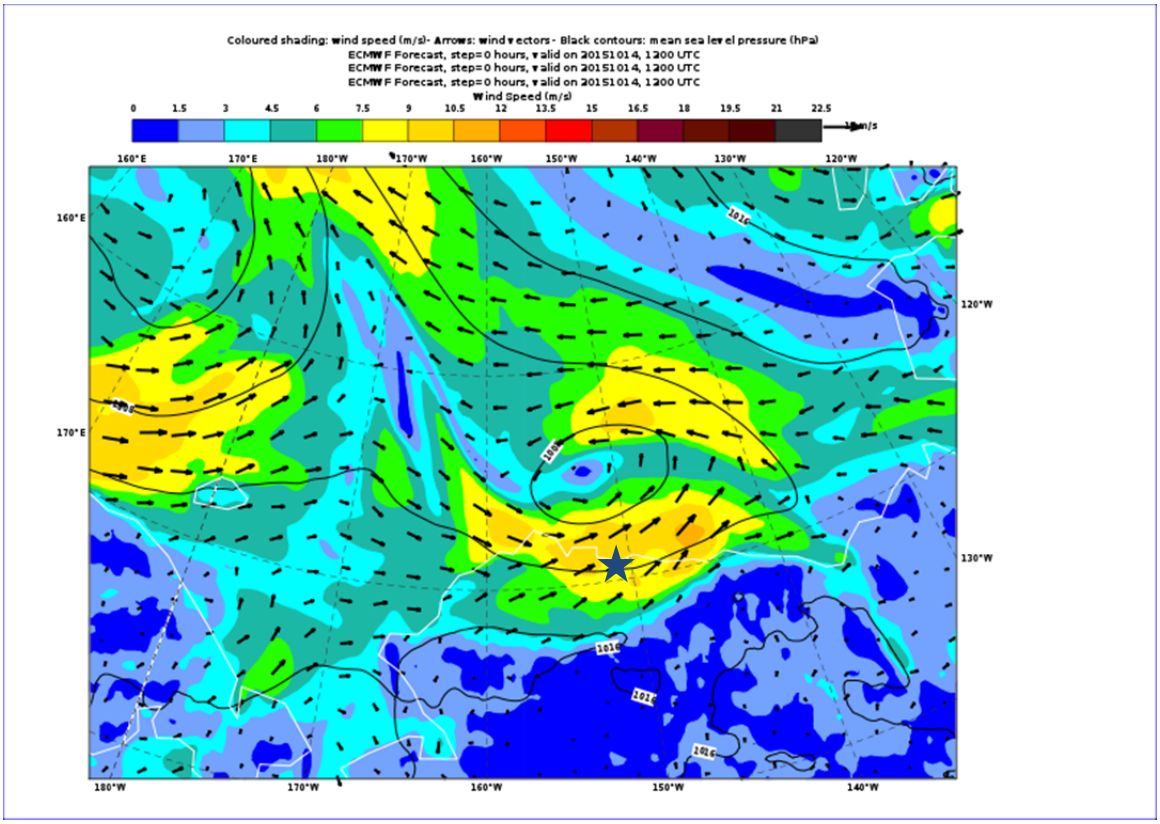


ECMWF forecast valid for 20151014 at 1200 UTC which was YD287, the fifth and final day of the YD285 event. This forecast was a 0 hour step from the initial model run. The ship location is denoted by the blue star. Winds are the 10m winds.

## 2. Visual Analysis

Soundings from the beginning of the wind event (YD 283) showed an atmospheric inversion (AI) at around 800 meters of 3˚ C (Figure 21). This AI would remain throughout the duration of the wind event until it was eventually broken up by the low pressure system moving into the area. The wind profile from YD 283 of the event (Figure 22) showed a weak but early jet below the inversion with a maximum wind speed of 8 m/s. The wind direction at this sounding is 100˚ which is both parallel to the ice edge and along the constant pressure line.

Figure 21. Temperature Profile from Sounding 15101023

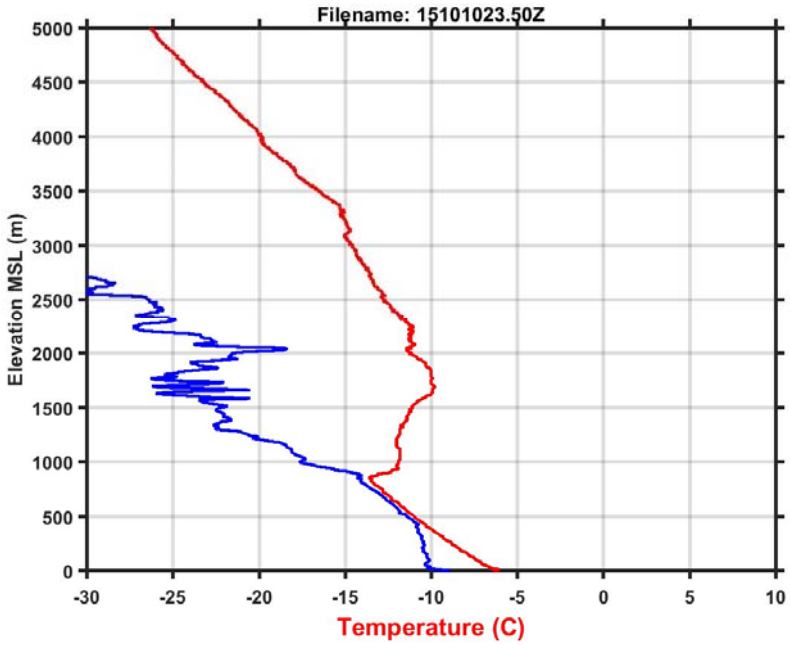


The temperature (red) and dew point (blue) profiles measured from the sounding taken on 151010 at 2330 UTC.

Figure 22. Wind Profile from Sounding 15101023

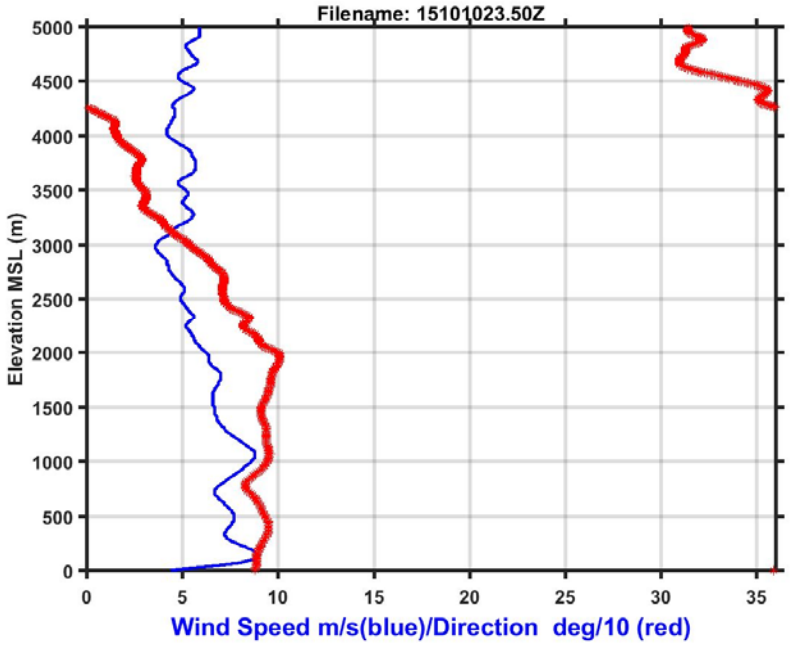


The wind direction (red) and wind speed (blue) profiles measured from the sounding taken on 151010 at 2330 UTC.

During the event the inversion maintained at a fairly constant height of around 800 meters. The soundings showed some variation in height that could be explained by the differing locations from which each sounding was taken. The temperature soundings from YD 285 show a similar height of the AI but it was slightly stronger, 5° C as opposed to 3° C (Figure 23). The wind for this sounding showed a LLJ with a maximum at around 800m which corresponds to the AI (Figure 24). The wind direction has shifted slightly but is still parallel to the ice edge and along a constant pressure line.

Figure 23. Temperature Profile from Sounding 15101200

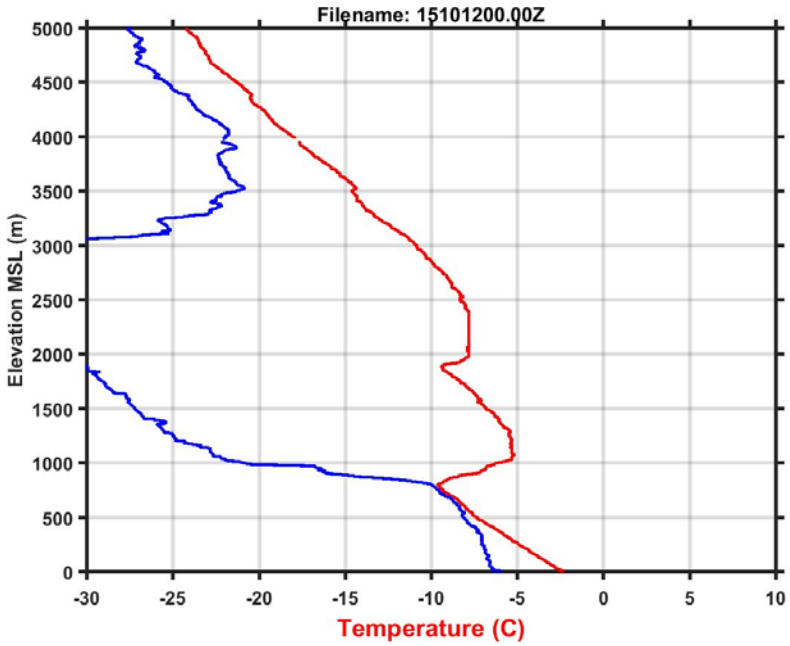


The temperature (red) and dew point (blue) profiles measured from the sounding taken on 151012 at 0000 UTC.

Figure 24. Wind Profile from Sounding 15101200

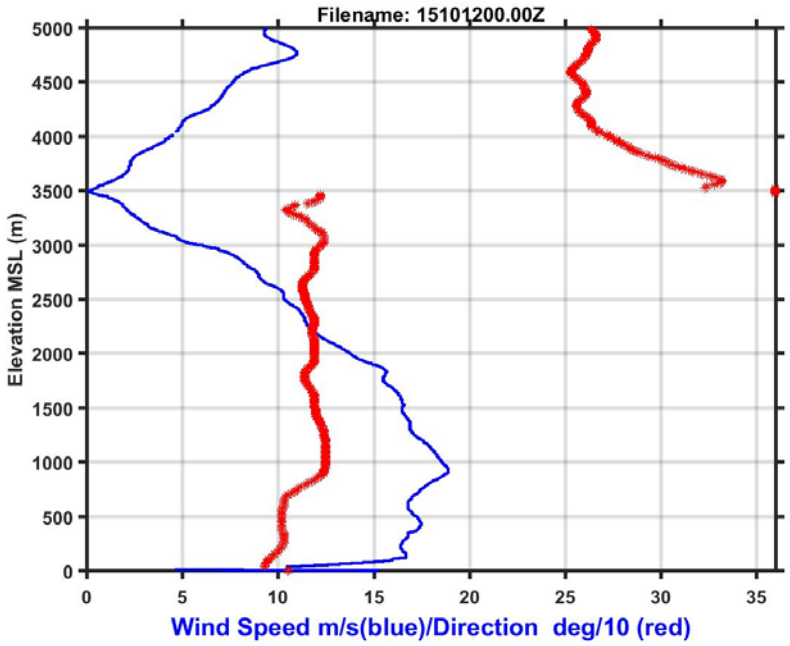


The wind direction (red) and wind speed (blue) profiles measured from the sounding taken on 151012 at 0000 UTC.

As the low moved into the area and disrupted the LLJ, the inversion first increased in height and eventually dissipated as a result of atmospheric mixing caused by the low pressure system. The soundings from YD 287 or day five of the event showed the inversion gone in the lower levels (Figure 25). The mixing of the atmosphere combined with the disruption of the pressure surface cause the jet to dissipate (Figure 26). The wind direction shifted away from easterly and is no longer parallel with the ice edge or flowing along a constant pressure surface.

Figure 25. Temperature Profile from Sounding 15101417

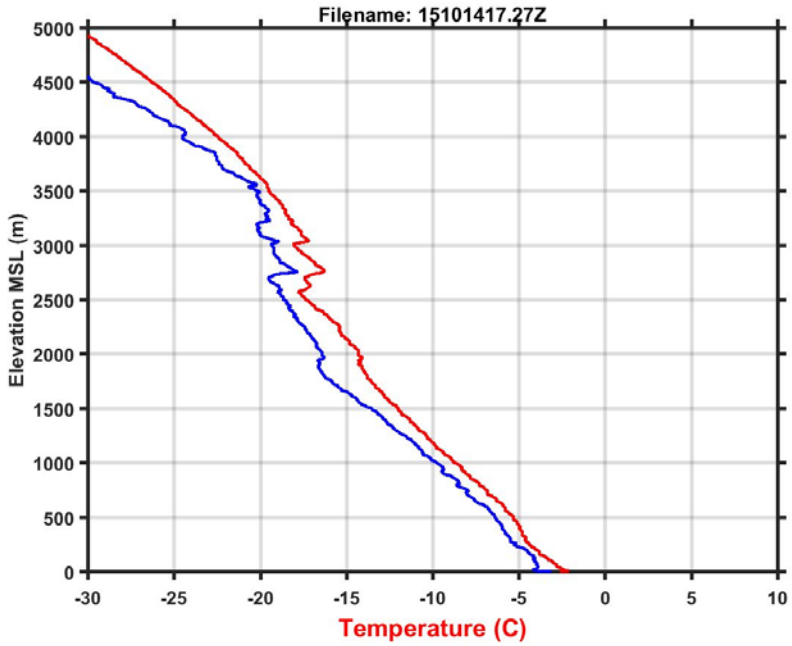


The temperature (red) and dew point (blue) profiles measured from the sounding taken on 151014 at 1716 UTC.

Figure 26. Winds Profile from Sounding 15101417

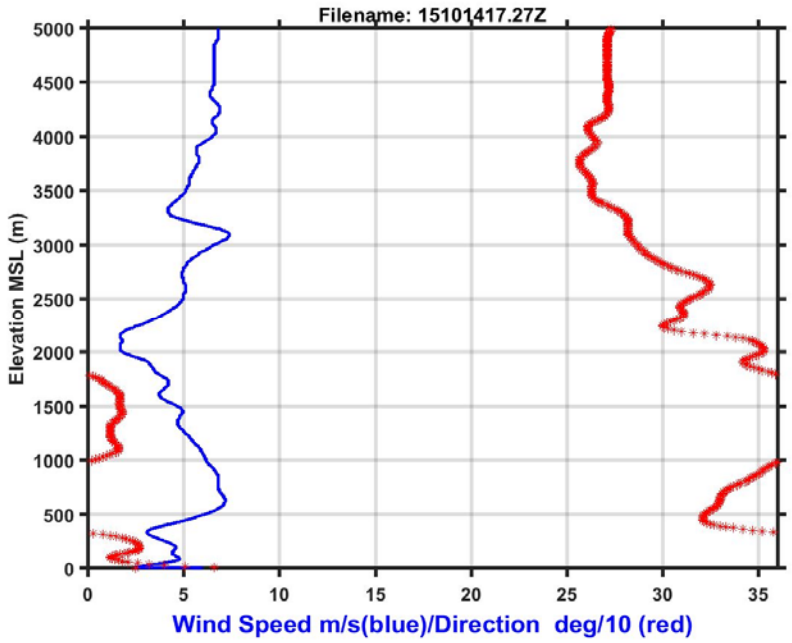


The wind direction (red) and wind speed (blue) profiles measured from the sounding taken on 151014 at 1716 UTC.

The visual analysis of the data from the YD 285 event showed few of the soundings were taken across the axis of the wind. To further explain, the wind being easterly, very few of the soundings were taken as the ship moved from north to south perpendicular to the wind direction. The importance of soundings taken across the wind axis is to verify gradients and allow for a fairly accurate calculation of the geostrophic wind via the thermal wind equation.

The best set of data for this purpose was from YD 286, which was when the jet was beginning to dissipate. The three soundings selected (15101305, 15101311, and 15101317) were collected as the ship transited to the southwest, not exactly perpendicular to the wind direction but close enough to obtain a cross section of the wind. The temperature profiles showed both warming and an increase in height of the AI, which is consistent with the ship traveling from north to south i.e. from relatively colder air to relatively warmer air (Figure 27). The temperature profiles also showed that the inversion was weakening which was consistent with the progression of the jet and its weakening.

Figure 27. Temperature Profiles from Soundings 15101305-15101317

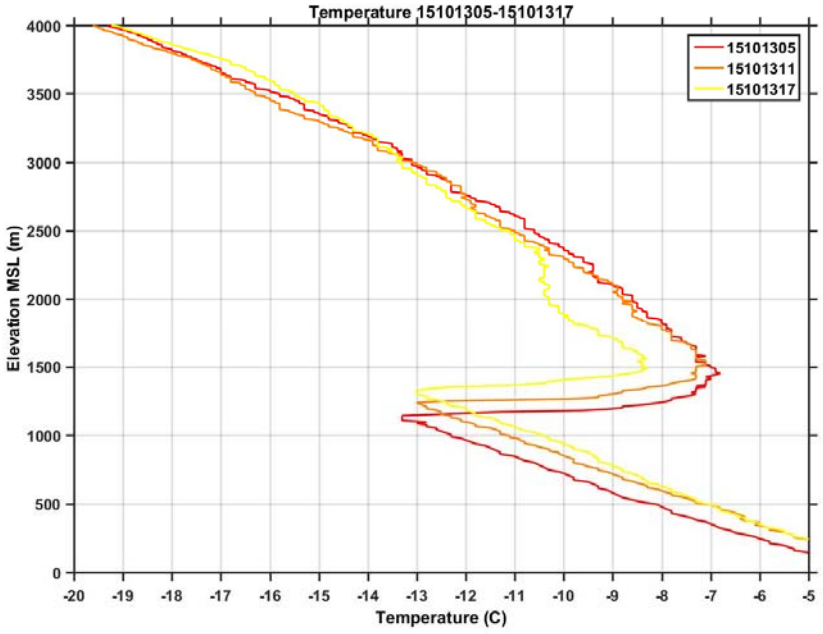


The temperature profiles from soundings 15101305, 15101311, 15101317 all show an AI between 1000m and 1500m. The profiles show the AI increasing in height and weakening over time.

The wind profiles from the same soundings (15101305, 15101311, and 15101317) showed the jet with a maximum at around 1000m or the AI height that drops off quickly as the inversion weakens (Figure 28). Some of the decrease in jet speed can be attributed to the ship moving to the south away from the area of strongest temperature gradient however; the jet was also weakening at this point.

Figure 28. Wind Profiles from Soundings 15101305-15101317

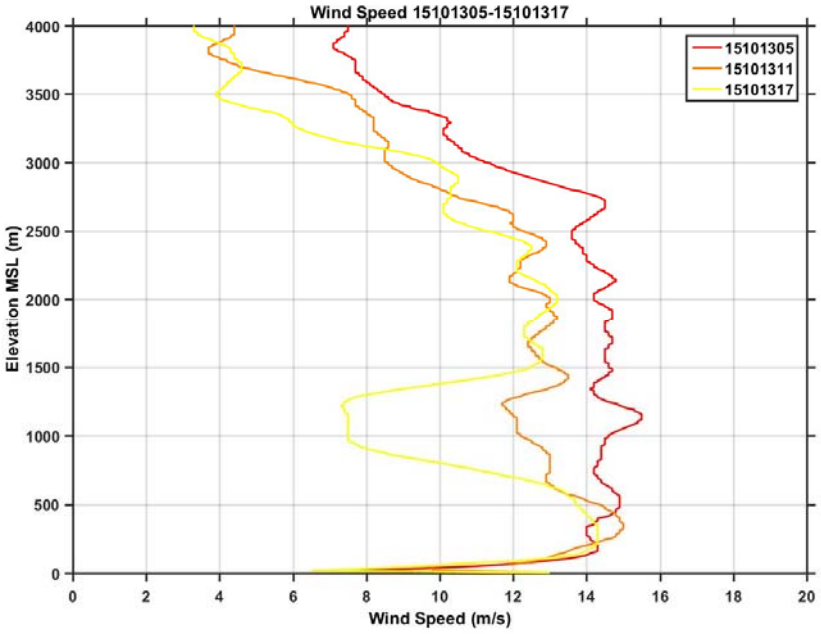


The wind speed profiles from soundings 15101305, 15101311, 15101317 show the jet max at just above 1000m during the first sounding and then dissipating over time.

### 3. Quantitative Analysis

The calculation of the geostrophic wind for this case was less accurate than desired due to the cross section of the jet not being perpendicular to the wind direction. The first calculation shows a very similar profile just differing in magnitude (Figure 29). It shows consist wind speeds above the inversion, a slight dip below the observed speeds at the inversion and then it increases to the surface. The increase toward the surface is due to the thermal wind equation not accounting for friction. The wind calculations between the other two locations showed similar characteristics, matching the wind speed

above the inversion, dropping below the observed wind speed at the AI (Figure 30 and Figure 31). These variations were again caused by the soundings not being taken exactly perpendicular to the wind axis.

Figure 29. Soundings 15101305 and 15101311

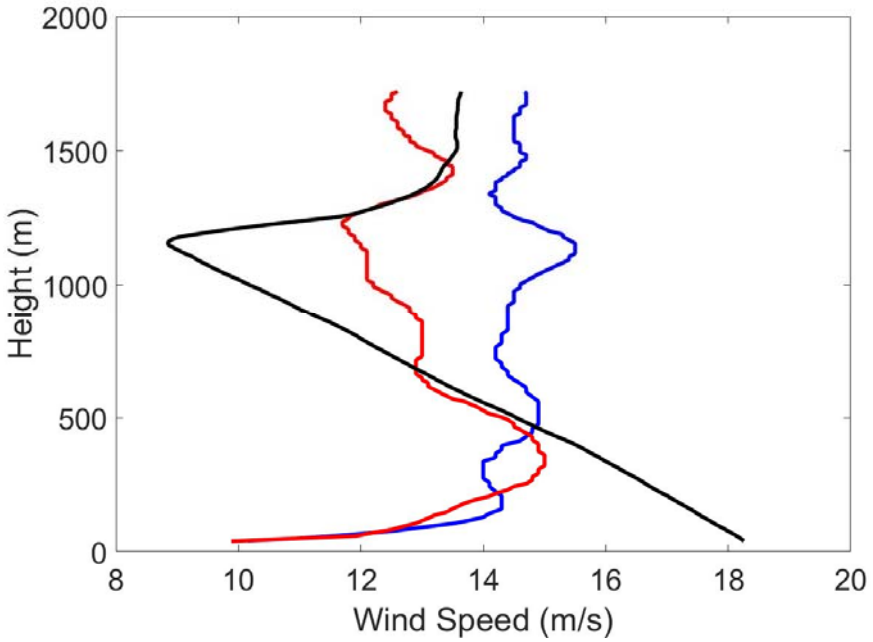


The blue line represents the 15101305 sounding wind speed and the red line represents the 15101311 sounding wind speed. The black line is the calculated geostrophic wind using the thermal wind equation and the gradient between the two sounding locations.

Figure 30. Soundings 15101311 and 15101317

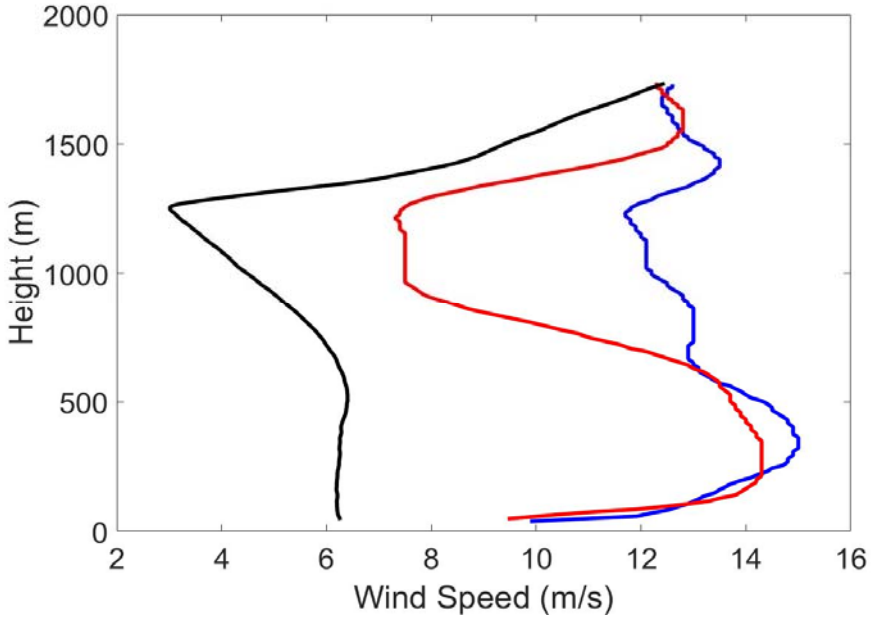


The blue line represents the 15101311 sounding wind speed and the red line represents the 15101317 sounding wind speed. The black line is the calculated geostrophic wind using the thermal wind equation and the gradient between the two sounding locations

Figure 31. Soundings 15101317 and 15101323

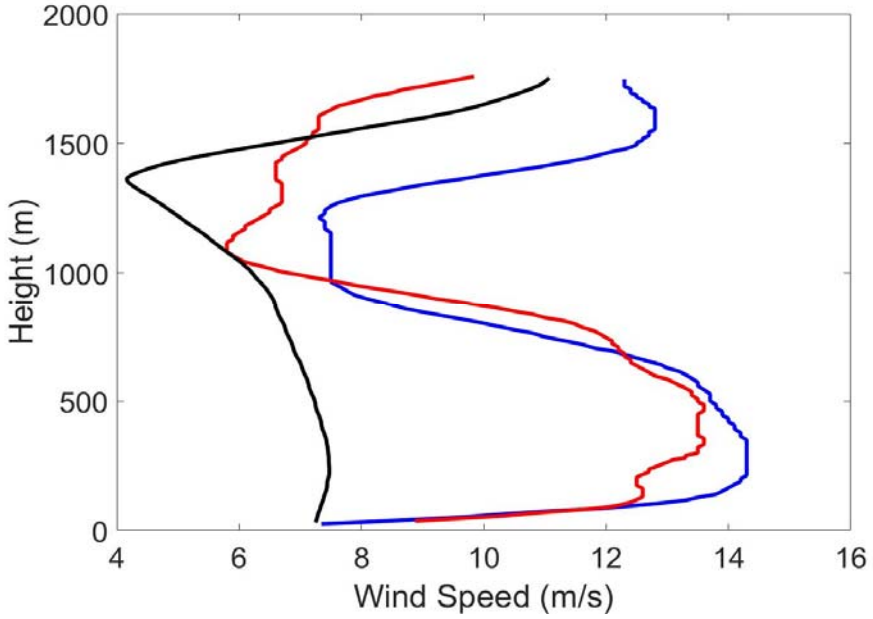


The blue line represents the 15101317 sounding wind speed and the red line represents the 15101323 sounding wind speed. The black line is the calculated geostrophic wind using the thermal wind equation and the gradient between the two sounding locations

In conclusion the synoptic situation during this event shows strong evidence of the jet being the result of baroclinicity. The ice edge and pressure surface are parallel and the temperature gradient is perpendicular, all of which are indicators of baroclinicity. The soundings were not definitive in showing the jet was the result of baroclinicity but they did further support the baroclinicity hypothesis.

## D. YEAR DAY 292 EVENT

### 1. Synoptic Situation

The YD 292 event had a dissimilar synoptic setup than the rest of the events in this thesis. The surface pressure was not aligned with the ice edge on YD 291 and remained that way throughout the event. The surface pressure was under the influence of a high pressure system moving into the research area from the northwest (Figure 32). The winds during this event are northeasterly at around 10 m/s, which is consistent with the sounding data. BY YD 292 the high pressure system reached the research area and was influencing the jet (Figure 33). It is likely that the approaching high pressure system changed both the surface pressure and the temperature gradient to no longer align with the ice edge but still allow for a relatively short and weak LLJ.

Figure 32. ECMWF Model Forecast valid October 18, 2015 at 1200 UTC

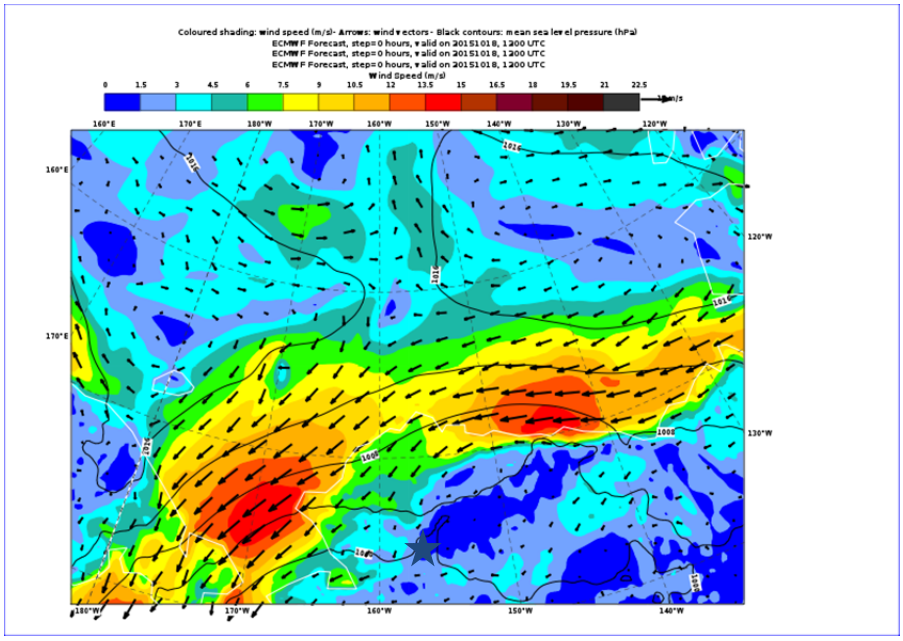


ECMWF forecast valid for 20151018 at 1200 UTC which is YD291, the first day of the YD292 event. This forecast is a 0 hour step from the initial model run. The ship location is denoted by the blue star. Winds are the 10m winds.

Figure 33. ECMWF Model Forecast valid October 19, 2015 at 1200 UTC

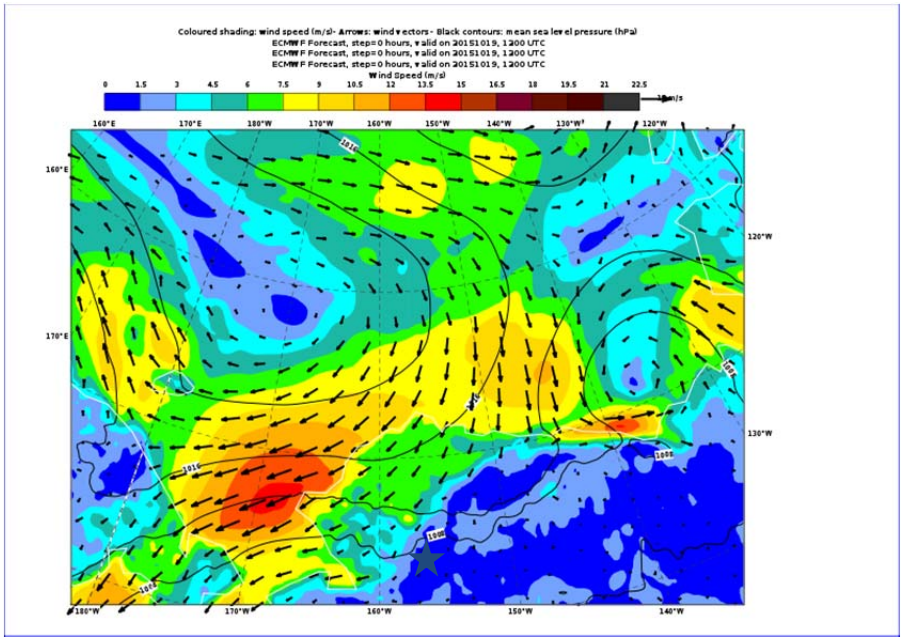


ECMWF forecast valid for 20151019 at 1200 UTC which is YD292, the SECOND day of the YD292 event. This forecast is a 0 hour step from the initial model run. The ship location is denoted by the blue star. Winds are the 10m winds.

## 2. Visual Analysis

The data for this event provided several soundings that were taken as the ship moved in to the north, not directly into the direction of the wind but not perpendicular to it. These soundings were collected as the event was dissipating and the wind speed profiles support this. The temperature soundings from those profiles showed that a gradient did exist though not as strong as in other cases. The AI height fluctuates between 250 m and 500 m gaining height and strength as the ship traveled north (Figure 34). The wind profiles for this event show the jet dissipating to less than 5 m/s by the end of the period which is also the conclusion of the event.

Figure 34. Temperature Profiles of Soundings 15101901-15101923

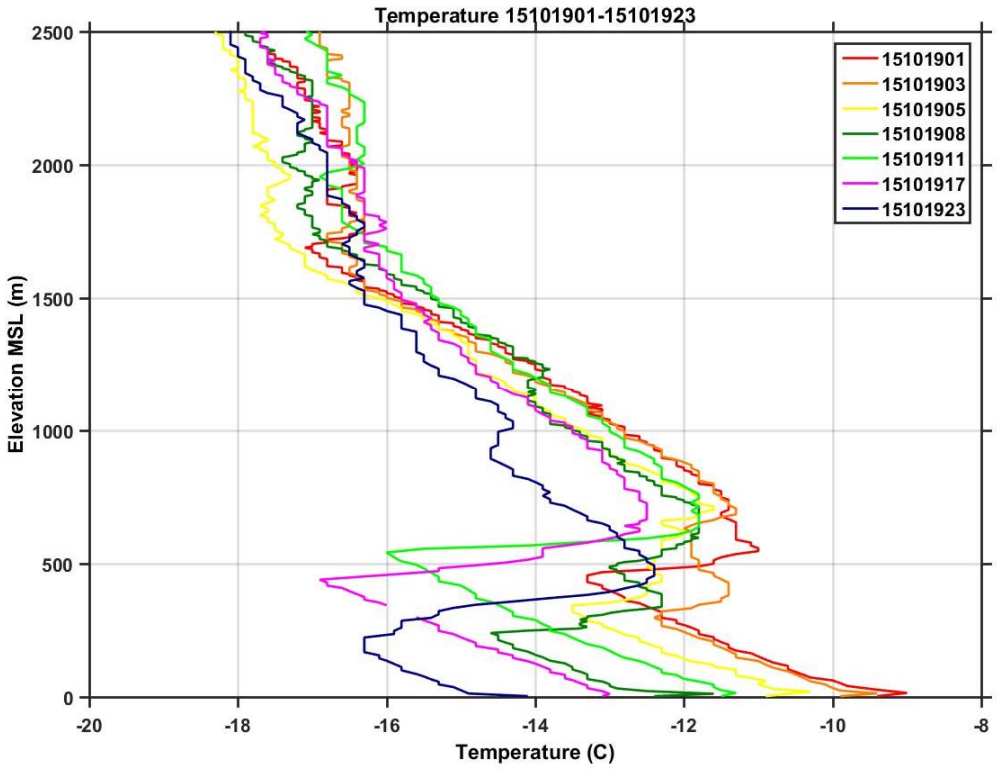


The temperature profiles from soundings 15101901, 15101903, 15101905, 15101908, 15101911, 15101917, 15101923 all show an AI between 250m and 550m.

Figure 35. Wind Speed Profiles of Soundings 15101901-15101923

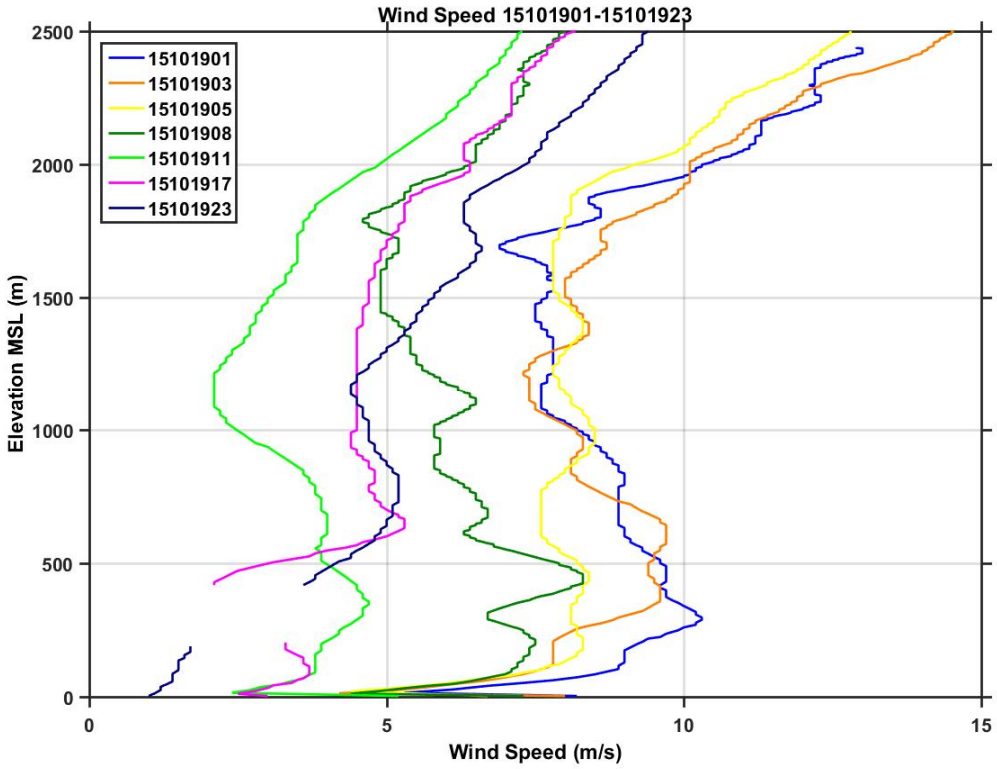


The temperature profiles from soundings 15101901, 15101903, 15101905, 15101908, 15101911, 15101917, 15101923 all show an AI between 250m and 550m.

## 3. Quantitative Analysis

The YD 292 event was the shortest event meaning that it also has the fewest soundings and of those soundings, only two were taken close enough to across the jet axis to be able to make a geostrophic wind calculation. The geostrophic wind was calculated between 15101903 and 15101905 and it showed a fairly close match to the profile with slightly higher wind speeds than observed (Figure 36). Some of the overestimate is likely due to the ship not transiting exactly perpendicular to the wind and the absence of friction in the thermal wind equation used to generate the profile.

Figure 36. Soundings 15101903 and 15101905

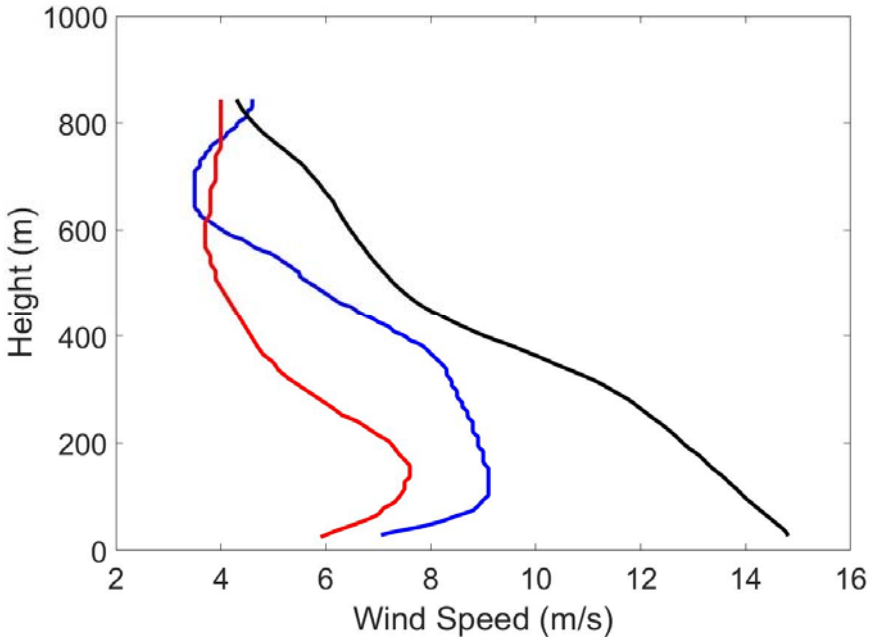


The blue line represents the 15101903 sounding wind speed and the red line represents the 15101905 sounding wind speed. The black line is the calculated geostrophic wind using the thermal wind equation and the gradient between the two sounding locations.

In conclusion, it is likely that this case was the result of baroclinicity that was being influenced by the high pressure system. In the other cases the surface pressure was aligned with the ice edge however in this case it appears to have been shifted as the high moves in. This is probably a contributing factor to why this event was both weaker in intensity and shorter in duration.

## E. YEAR DAY 297 EVENT

### 1. Synoptic Situation

The YD 297 event began when the entire region was under the influence of a high pressure system that is positioned to the Northeast of the research area (Figure 37). The winds are out of the east in the research area and are in the 10-12m/s wind speed category. The wind speed and direction were consistent with soundings taken during this time, the maximum speeds of the wind event were observed toward the end of YD 297 and in the early hours of YD 297. Based on the orientation of the surface pressure, ice

edge, and relative wind direction, the preliminary assumption was that this jet was the result of baroclinicity.

Figure 37. ECMWF Model Forecast valid October 23, 2015 at 1200 UTC

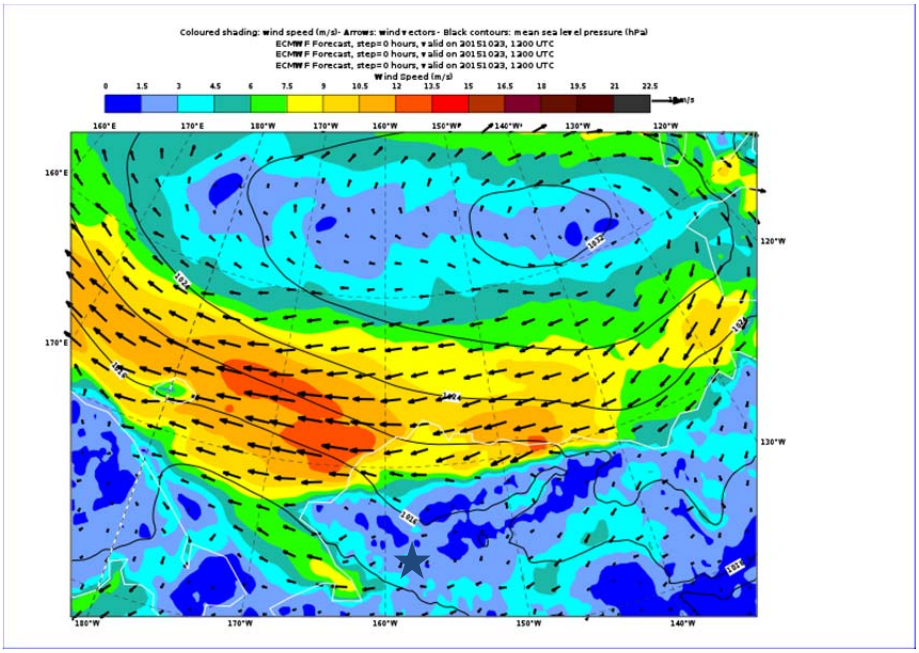


ECMWF forecast valid for 20151023 at 1200 UTC which was YD296, the first day of the YD285 event. This forecast was a 0 hour step from the initial model run. The ship location is denoted by the blue star. Winds are the 10m winds.

As the high pressure system moves out of the area the pressure surface remains organized north to south and the winds remain out of the east (Figure 38). The winds at this point were beginning to dissipate but are still strong. The pressure surface was still oriented north to south but it was beginning to disorganize downstream.

Figure 38. ECMWF Model Forecast valid October 24, 2015 at 1200 UTC

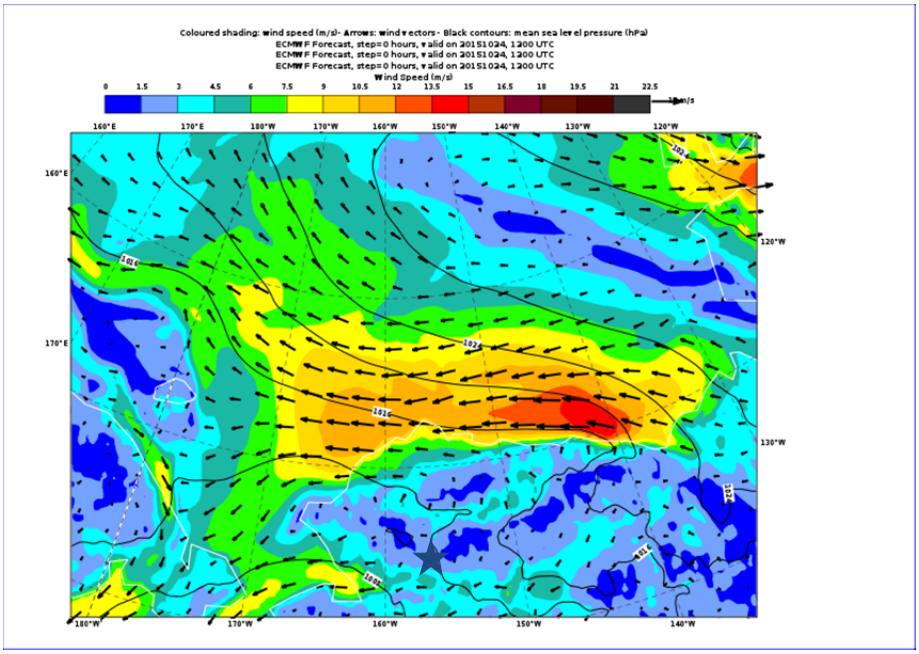


ECMWF forecast valid for 20151024 at 1200 UTC which was YD297, the second day of the YD297 event. This was also the day with the strongest winds. This forecast was a 0 hour step from the initial model run. The ship location is denoted by the blue star. Winds are the 10m winds.

By YD 298 the surface pressure continued to shift and was no longer parallel to the ice edge. No well-organized high pressure or low pressure system was present in the area, however relative high and low pressure were altering the synoptic situation. The jet dissipated rapidly as the surface pressure changed and by YD 298 was no longer present. The winds both reduced in speed and changed direction (Figure 39).

Figure 39. ECMWF Model Forecast valid October 25, 2015 at 1200 UTC

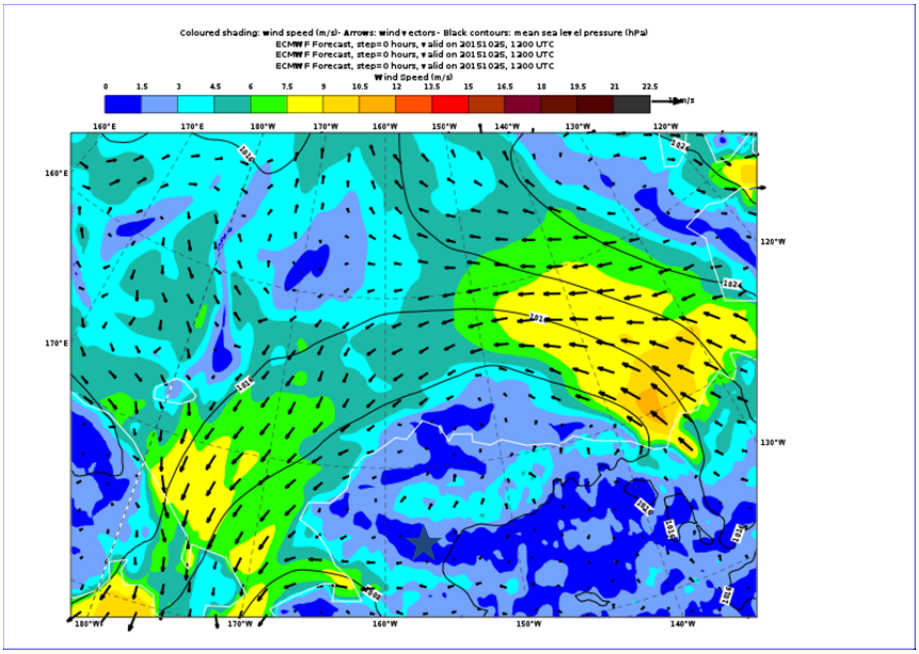


ECMWF forecast valid for 20151024 at 1200 UTC which was YD298, the third and final day of the YD297 event. This forecast was a 0 hour step from the initial model run. The ship location is denoted by the blue star. Winds are the 10m winds.

## 2. Visual Analysis

For the visual analysis of soundings as the jet was building the ship was moving to the southwest nearly perpendicular to the direction of the jet. This allowed for a side by side comparison of the soundings as the jet was intensifying. The soundings shown in (Figure 40) were all taken as the jet moved to the south. As the ship moved to the south the inversion increased in height (100m to 300m), consistent with having warmer temperatures at the surface but remained about the same intensity. These soundings also showed a strong gradient temperature from north to south and coupled with the surface pressure from (Figure 37) were ideal baroclinic conditions for the jet to develop.

Figure 40. Temperature Profiles from Soundings 15102306-15102316

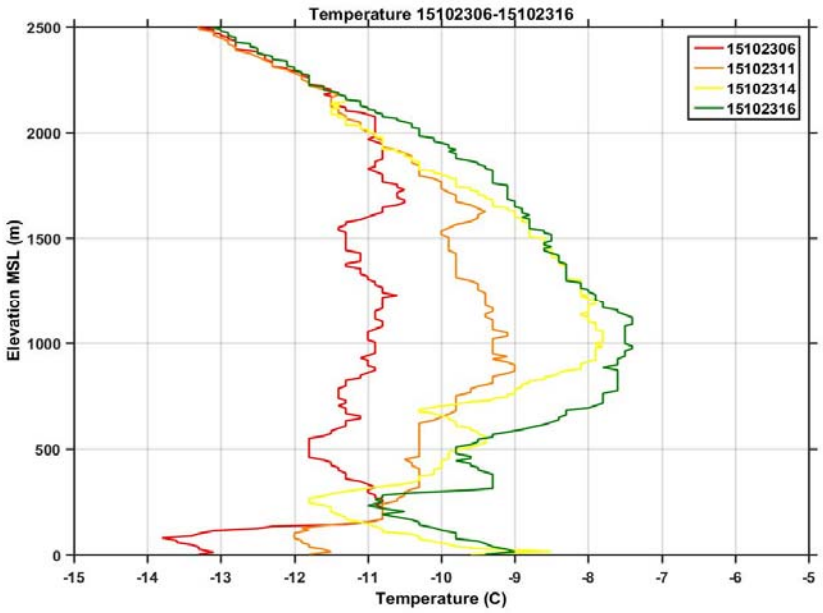


The temperature profiles from soundings 15102306, 15102311, 15102314, and 15102316 all show an AI between 100m and 250m. The profiles show the AI increasing in height over time.

The jet speed maximum matched the height of the AI at each sounding and increase from one sounding to the next with the exception being sounding 15102314 (Figure 41). The 15102314 sounding was only slightly stronger than the 15102316 sounding and this could have been caused by a relative gust within the jet or because of the change in location from one sounding to the next. These profiles supported the assumption that this jet was the result of baroclinicity.

Figure 41. Wind Profiles form Soundings 15102306-15102316

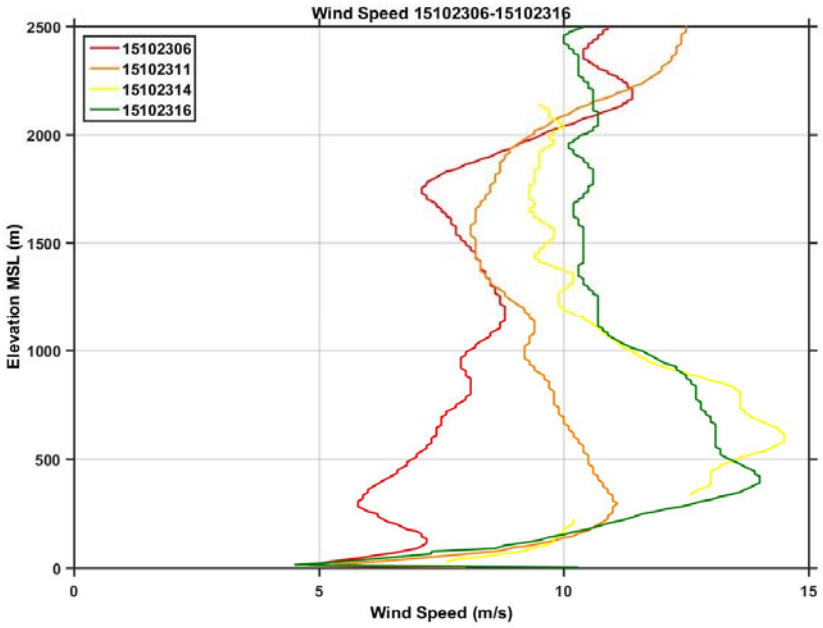


The wind speed profiles from soundings 15102306, 15102311, 15102314, and 15102316 show the jet max increasing in height and intensity over time.

### 3. Quantitative Analysis

The modeling of the geostrophic wind for this case was simplified by the orientation of the soundings taken across the axis of the wind direction. However, the relative low height of this jet meant that more of the interest area was under the effects of friction which is not accounted for in the thermal wind equations used to model geostrophic winds. The first calculation between 15102306 and 15102311 had the geostrophic wind matching the observed wind above the AI and then increasing to the surface at higher wind speeds than the observed (Figure 42). This is likely due to the impacts of friction.

Figure 42. Soundings 15102306 and 15102311

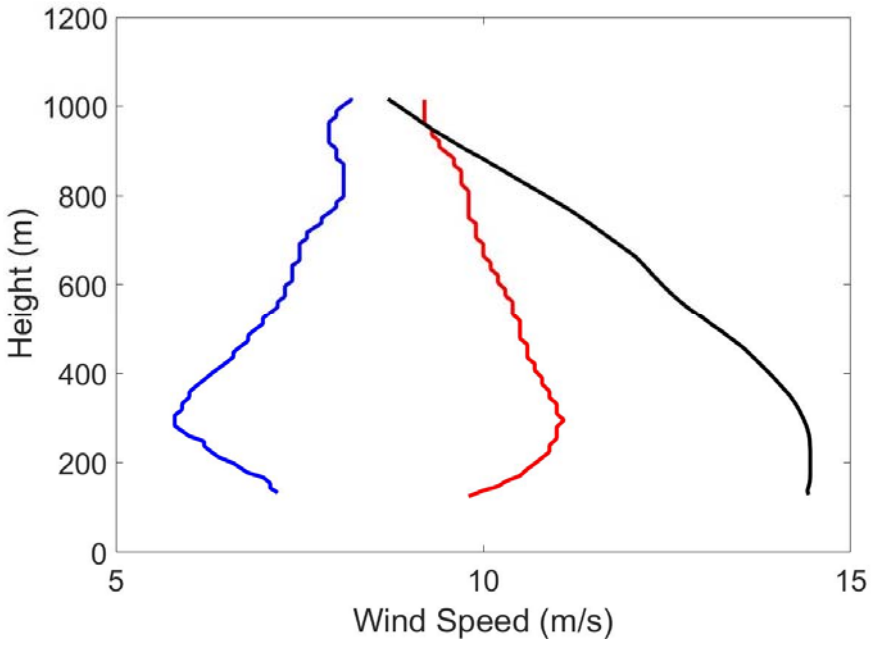


The blue line represents the 15102306 sounding wind speed and the red line represents the 15102311 sounding wind speed. The black line is the calculated geostrophic wind using the thermal wind equation and the gradient between the two sounding locations

The second calculation of geostrophic wind between 15102311 and 15102314 had a similar profile to the observed winds and fell in between for wind speed which is to be expected since the geostrophic wind calculation is an average of the wind between the two soundings. The geostrophic calculation does show much higher speeds at the surface than the observed but that is again due to the lack of friction (Figure 43). This profile makes a strong case for the LLJ being the result of baroclinicity since the calculated geostrophic wind is a good fit to the observed wind.

Figure 43. Soundings 15102311 and 15102314

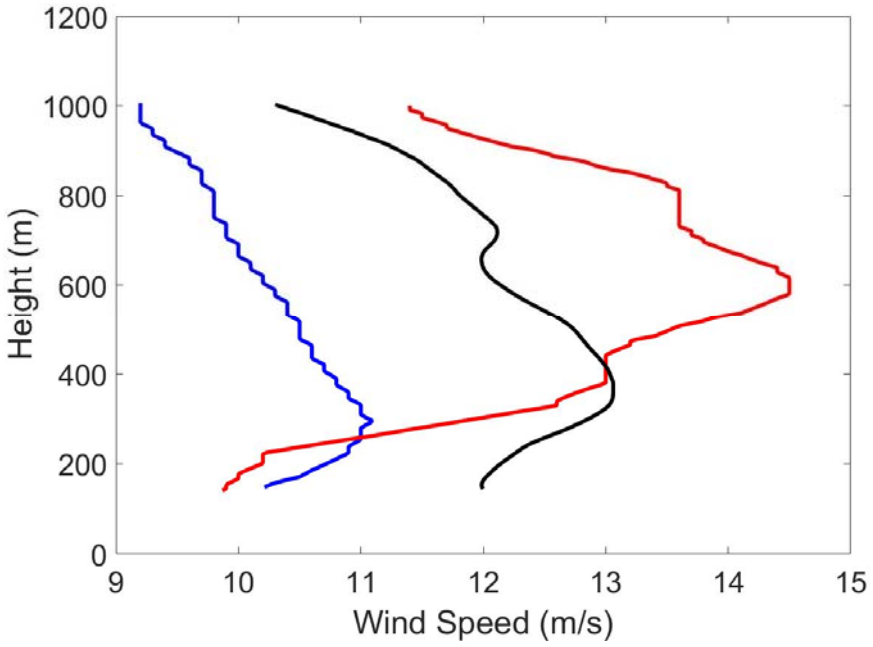


The blue line represents the 15101311 sounding wind speed and the red line represents the 15101314 sounding wind speed. The black line is the calculated geostrophic wind using the thermal wind equation and the gradient between the two sounding locations

The third calculation of geostrophic wind between 15102314 and 15102316 showed a strong match above the inversion, a similar height for the jet maximum, and then steadily increasing to the surface at wind speeds above that of the observations (Figure 44). Some of the near surface increase is due again to no friction. These soundings were also taken at a time when the ship was traveling slightly less perpendicular to the wind direction than the previous two soundings which could also account for the mismatch.

Figure 44. Soundings 15102314 and 15102316

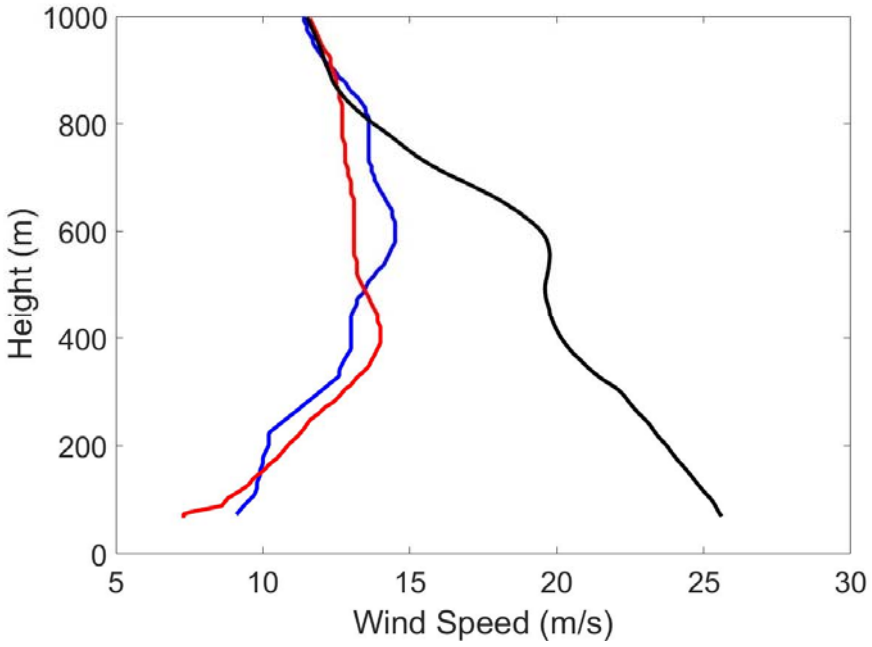


The blue line represents the 15102314 sounding wind speed and the red line represents the 15102316 sounding wind speed. The black line is the calculated geostrophic wind using the thermal wind equation and the gradient between the two sounding locations

In conclusion this event shows strong evidence of being the result of baroclinicity. The orientation of the ice edge, temperature gradient, and pressure surface all are indicators of baroclinicity. The soundings further supported the baroclinicity hypothesis.

## F. YEAR DAY 307 EVENT

### 1. Synoptic Situation

During the beginning (YD 305) of the YD307 event the research area was under the influence of a high pressure system located to the northeast (Figure 45). The only relatively high winds are near a weak low to the west of the research area. The pressure gradient is fairly disorganized and is not aligned with the ice edge. The research area show winds between 9 m/s and 10.5 m/s out of the southeast, which was consistent with soundings taken during that time.

Figure 45. ECMWF Model Forecast valid November 1, 2015 at 1200 UTC

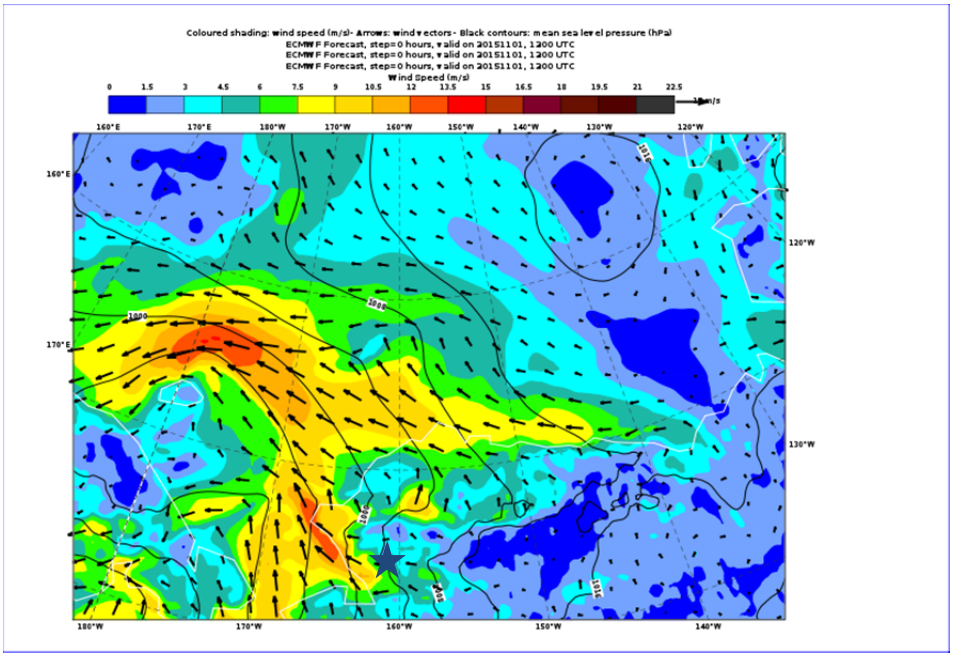


ECMWF forecast valid for 20151101 at 1200 UTC which was YD305, the first day of the YD307 event. This forecast was a 0 hour step from the initial model run. The ship location is denoted by the blue star. Winds are the 10m winds.

The pressure systems both moved out of the area and by YD 306 and the pressure gradient organized and aligned itself north south, relatively parallel to the ice edge (Figure 46). During this time winds increased and shifted from southeast to east. The winds on the ECMWF model indicated jet speeds of around 13 m/s to 14.5 m/s, which was slightly less than observed from the soundings. The wind direction at the surface remained easterly which was consistent with the sounding data from this time period. This synoptic setup remained in place for both YD 306 and YD 307 (Figure 46 and Figure 47) and the associated jet also maintained nearly constant speed and direction over that same time period.

Figure 46. ECMWF Model Forecast valid November 2, 2015 at 1200 UTC

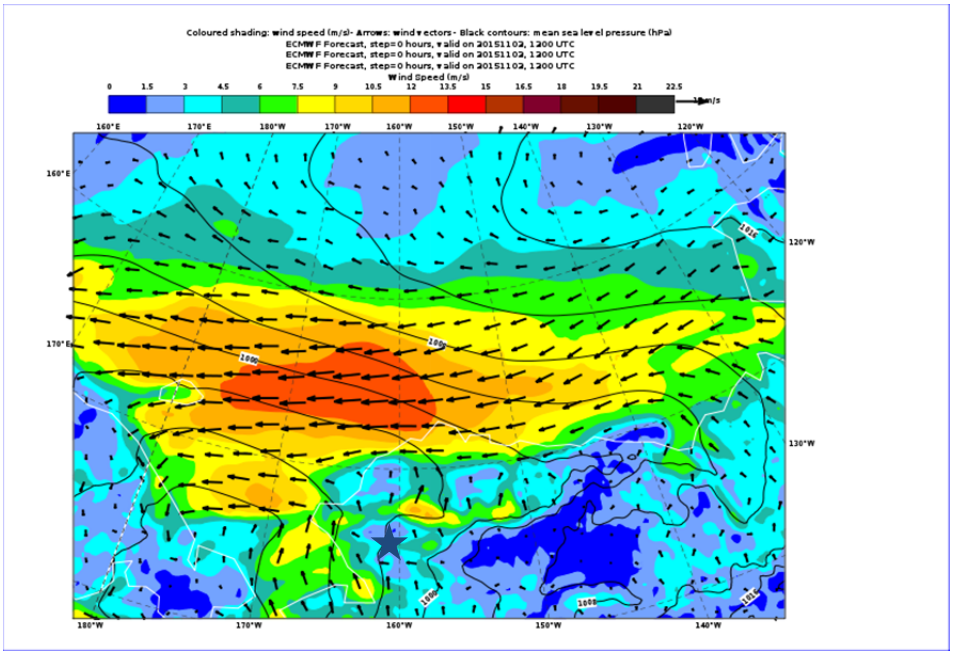


ECMWF forecast valid for 20151102 at 1200 UTC which is YD306, the second day of the YD307 event. This forecast was a 0 hour step from the initial model run. The ship location is denoted by the blue star. Winds are the 10m winds.

Figure 47. ECMWF Model Forecast valid November 3, 2015 at 1200 UTC

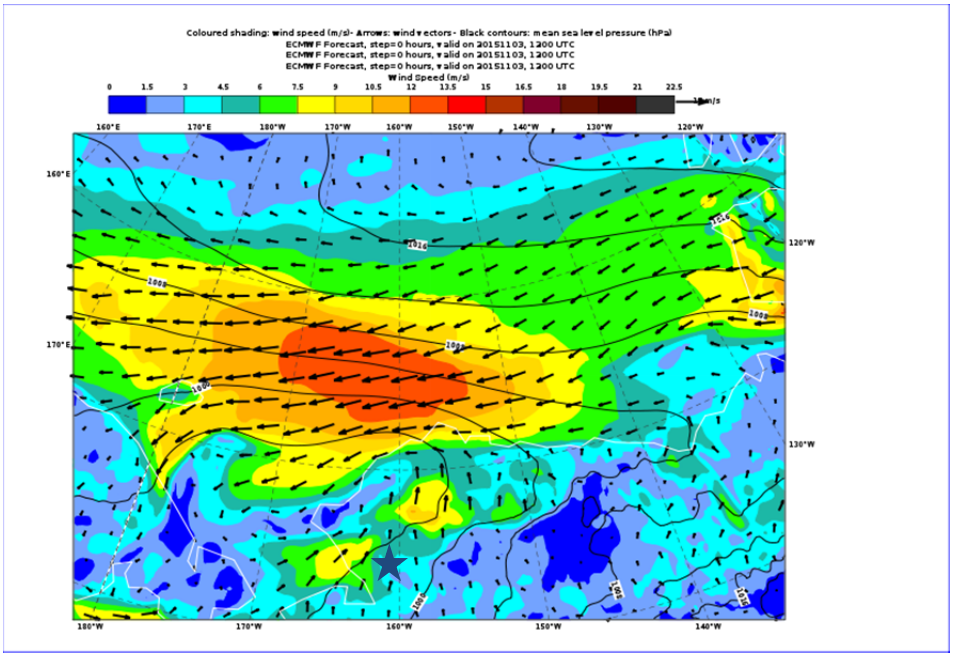


ECMWF forecast valid for 20151103 at 1200 UTC which was YD307, the third day of the YD307 event. This was also the day of the strongest observed winds. This forecast was a 0 hour step from the initial model run. The ship location is denoted by the blue star. Winds are the 10m winds.

On YD 308 the pressure surface shifted and the jet changed direction and reduced in speed (Figure 48). There were no strong low or high pressure systems that made their way into the area. However, there was a relatively weak low that moved into the northern most parts of Alaska that contributed to the alteration of the surface pressure and caused the jet to dissipate slowly over YD308 and YD309 (Figure 48 and 49). The winds decreased and the direction shifted from easterly to north easterly which was consistent with the soundings.

Figure 48. ECMWF Model Forecast valid November 4, 2015 at 1200 UTC

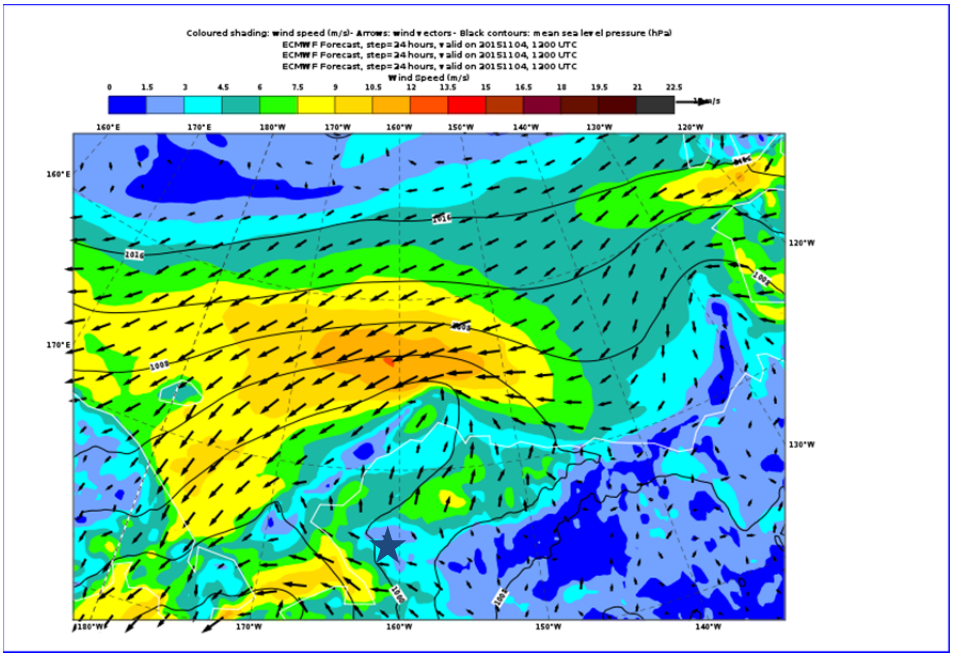


ECMWF forecast valid for 20151104 at 1200 UTC which is YD308, the fourth day of the YD307 event. This forecast was a 24 hour step from the initial model run. The ship location is denoted by the blue star. Winds are the 10m winds.

Figure 49. ECMWF Model Forecast valid November 5, 2015 at 1200 UTC

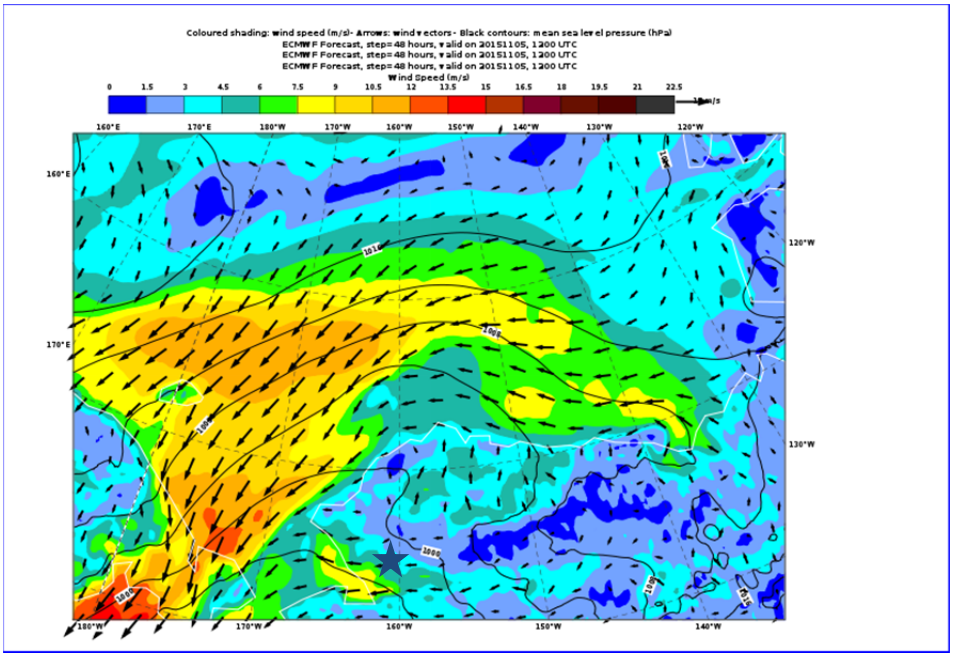


ECMWF forecast valid for 20151105 at 1200 UTC which was YD309, the fifth and final day of the YD307 event. This forecast was a 48 hour step from the initial model run. The ship location is denoted by the blue star.

The synoptic conditions present during this event lead to the initial hypothesis that this event is the result of baroclinicity driving a strong geostrophic wind. During the strongest wind days, the wind direction was along a constant surface pressure, and parallel to the ice edge meaning that it was likely also perpendicular to the temperature gradient.

## 2. Visual Analysis

Of the soundings taken during this event, six were taken while the ship transited to the south, perpendicular to the jet axis. These soundings were taken as the jet was beginning to weaken but still gave a good depiction of the AI and gradients. The temperature profiles (15110403, 15110407, 15110410, 15110413 15110416, 15110420) generally showed increasing surface temperatures and an increasing AI height consistent with the ship transiting to the south (Figure 50). The AI height increases from around 400m in the northern most sounding to 600m in the southern most sounding. This verified the presence of a temperature gradient from north to south.

Figure 50. Temperature Profiles from Soundings 15110403-15110420

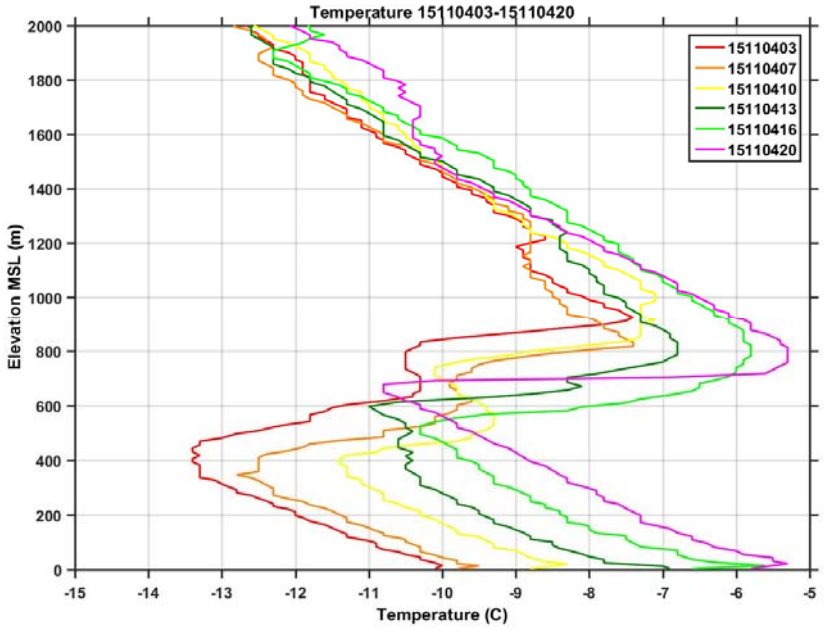


The temperature profiles from soundings 15110403, 15110407, 15110410, 15110413 15110416, and 15110420 all show an AI between 300m and 800m. The profiles show the AI increasing in height over time.

The wind profiles from the same soundings (15110403, 15110407, 15110410, 15110413 15110416, 15110420) shows the jet decreasing in speed over time and as the ship moves south (Figure 51). The jet maximum matches the AI height during the first sounding however, as the jet weakens, the max height decreases while the AI height increases. These soundings correlated well with the temperature soundings and further suggested that this jet was likely the result of baroclinicity.

Figure 51. Wind Speed Profiles from Soundings 15110403-15110420

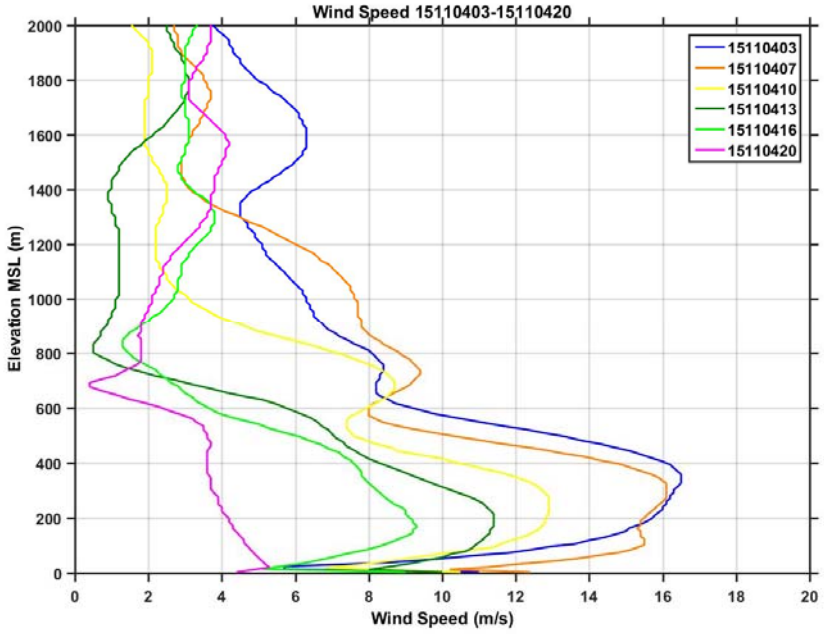


The wind speed profiles from soundings 15110403, 15110407, 15110410, 15110413 15110416, and 15110420 all show the jet max decreasing in height and intensity over time.

### 3. Quantitative Analysis

Due to the direction the ship was traveling during the soundings plotted in (Figure 50 and Figure 51), (15110403, 15110407, 15110410, 15110413 15110416, 15110420) the geostrophic wind calculations required little inference on the possible effects of the soundings not being taken across the axis of the jet. The geostrophic wind calculation from the first two soundings (Figure 52) showed a near identical wind profile to the observations only deviating near the surface where the effects of friction were not accounted for.

Figure 52. Soundings 15110403 and 15110407

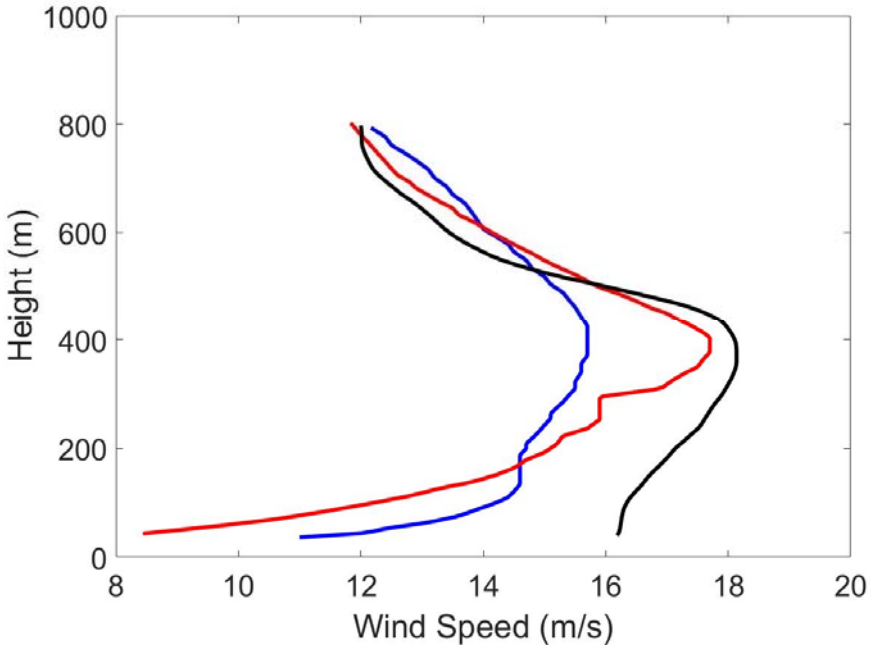


The blue line represents the 15110403 sounding wind speed and the red line represents the 15110407 sounding wind speed. The black line is the calculated geostrophic wind using the thermal wind equation and the gradient between the two sounding locations.

Similar to the soundings in (Figure 52), the geostrophic wind profile in (Figure 53 and Figure 54 and Figure 55 and Figure 56) also produced a near identical match to the observed winds. With each of these soundings the profile and wind speed matched almost identically only deviating near the surface where friction takes effect. These five soundings provided excellent support for the hypothesis that this jet was the result of baroclinicity.

Figure 53. Soundings 15110407 and 15110410

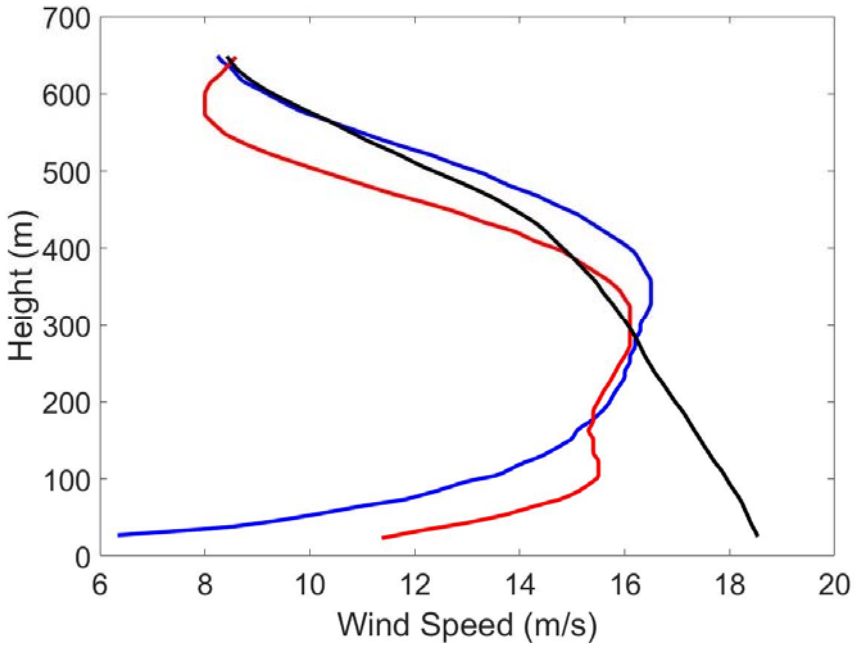


The blue line represents the 15110407 sounding wind speed and the red line represents the 15110410 sounding wind speed. The black line is the calculated geostrophic wind using the thermal wind equation and the gradient between the two sounding locations

Figure 54. Soundings 15110410 and 15110413

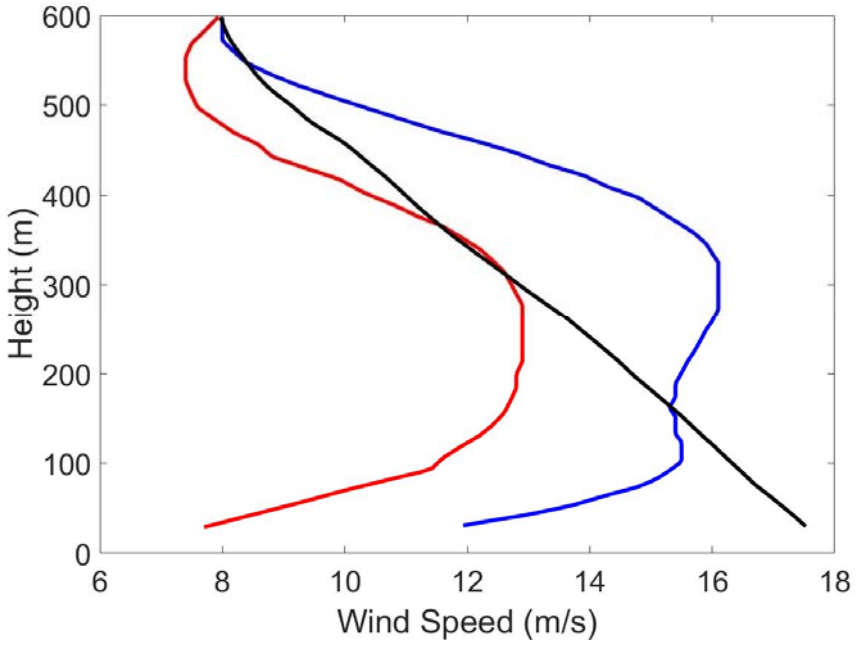


The blue line represents the 15110410 sounding wind speed and the red line represents the 15110413 sounding wind speed. The black line is the calculated geostrophic wind using the thermal wind equation and the gradient between the two sounding locations

Figure 55. Soundings 15110413 and 15110416

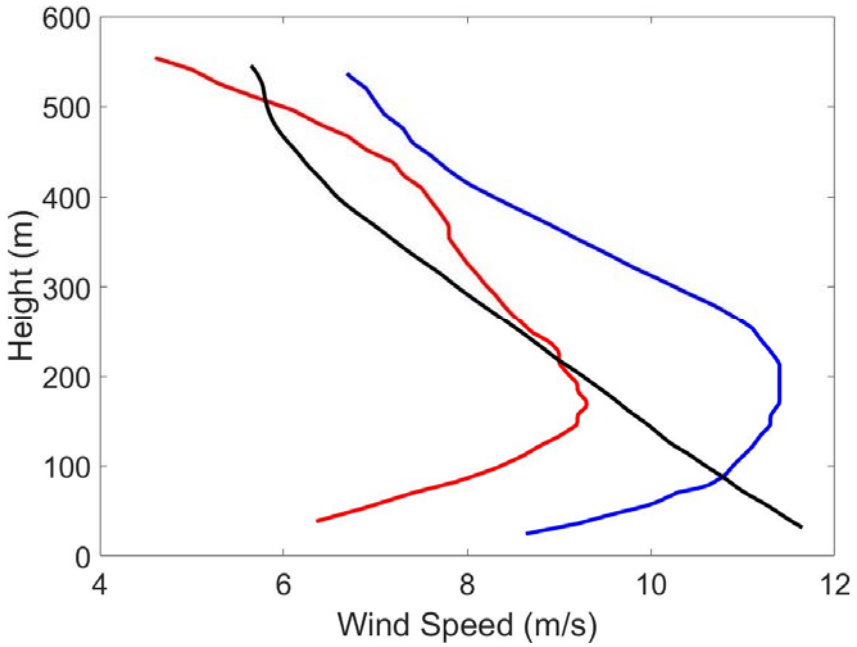


The blue line represents the 15110413 sounding wind speed and the red line represents the 15110416 sounding wind speed. The black line is the calculated geostrophic wind using the thermal wind equation and the gradient between the two sounding locations.

Figure 56. Soundings 15110416 and 15110420

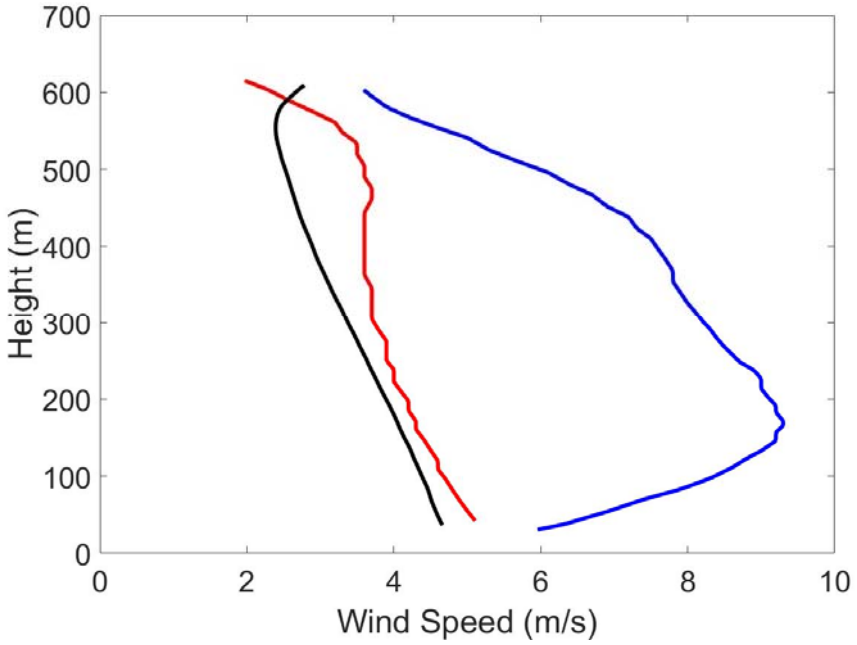


The blue line represents the 15110416 sounding wind speed and the red line represents the 15110420 sounding wind speed. The black line is the calculated geostrophic wind using the thermal wind equation and the gradient between the two sounding locations.

Based on the synoptic setup and the sounding data it is likely that this jet was the result of baroclinicity. The orientation of the surface pressure along with the temperature gradient and ice edge and the direction that the winds were flowing indicate low level baroclinicity was the cause of the LLJ. The soundings further supported the baroclinicity hypothesis by confirming the temperature gradient and showing that the wind profile was consistent with the temperature gradient.

# V. CONCLUSIONS AND RECOMMENDATIONS

## A. CONCLUSIONS

After studying four separate arctic LLJ events that all had different durations and intensities, the research has shown that all four events were likely the result of low level baroclinicity. All but one event had winds flowing alongside an ice edge, with the warm air to the left looking downwind. This situation results in an increasing geostrophic wind speed toward the surface. Friction in the lowest levels slows down the actual wind, resulting in a LLJ in the baroclinic region. The changing ice conditions in the ice edge region causes more heat to be added toward the open ocean side of the ice edge region, resulting in the observed horizontal temperature gradients. Once the wind direction is no longer aligned with the ice edge the temperature gradient disappears and ends the LLJ event.

In past years relatively light winds were measured throughout the fall in the Beaufort Sea and Chukchi sea region, for example during the SHEBA project (Guest, 2016). During the Sea State 2015 cruise, the winds were shown to be much more dynamic and included LLJ events. As the Arctic enters a new climate regime, the conditions observed during 2015 may be more common and thus LLJs may become a common occurrence in this region. The changing Arctic has caused the area in which the research was conducted to become a MIZ during the fall time period. In the past, this area had been predominantly solid ice pack. The presence of a MIZ versus solid ice pack will likely lead to an increase in the number of LLJ events in the Arctic.

LLJs also have an impact on the sea ice over which they occur. The strong winds can lead to sea swell and general ice movement. This motion can lead to the breakup and reduction of sea ice. The wind events can also cause ocean mixing which can bring warmer water to the surface and further contribute to sea ice melt. These conclusions are important to an organization like the US Navy who looks to operate more frequently in the Arctic region in the coming years.

## B. RECOMMENDATIONS

With the US Navy's desire to operate in the Arctic on a more frequent basis, more research into LLJs and Arctic weather are warranted. LLJs should be a consideration for any vessel or aviation asset in the Arctic because of the risk they pose to operations. However, their effects on sea ice and the ability to reduce and eliminate sea ice could be of tactical advantage to ships with limited ice breaking capabilities. Understanding when and why they occur could provide an advantage for operating within the MIZ. More research in the area could aid in safer operations and additional environmental exploitation.

One of the hindrances in accurately calculating the geostrophic wind was a lack of soundings that were taken consecutively and perpendicular to the wind axis. If another research cruise was to be conducted it would be helpful to drive the ship perpendicular to the wind during each wind event and launch soundings on a frequent basis for the entire duration of the event. This would simplify the calculation for the geostrophic wind and reduce the amount of inference that has to be made when accounting for data not being perpendicular to the wind axis.

# LIST OF REFERENCES


Andreas, E. L., K. J. Claffey, and A. P. Makshtas, 2000: Low-level atmospheric jets and inversions over the western Weddell Sea. *Bound.-Layer Meteor.,* **97,** 459–486.

Blackadar, A. K., 1957: Boundary layer wind maxima and their significance for the growth of nocturnal inversions. *Bull. Am. Meteorol. Soc.,* **38,** 283–290.

Guest, P. S., 2016: Personal communication regarding Arctic meteorology.

Holton, J. R., 1966: The diurnal boundary layer wind oscillation above the sloping terrain. *Tellus,* **XIX**, 2.

Holton, J. R., 2004: The Thermal Wind. *An Introduction to Dynamic Meteorology,* R. Dmowska, Ed. H. Rossby, Ed. International Geophysics Series No. **88**, Elsevier Academic Press, 70–75.

Jakobson, L., T. Vihma, E. Jakobson, T. Palo, A. Mannik, and J. Jaagus, 2013: Low-level jet characteristics over the Arctic Ocean in Spring and Summer. *Atmos. Chem. Phys.,* **13**, 11089-11099, doi:10.5194/acp-13-11089-2013

Kozo, T. L., 1982: An Observational Study of Sea Breezes Along the Alaskan Beaufort Sea Coast: Part1. *J. Appl. Meteor.,* **21**, 891–905.

Lanfland, R., P. Tag, and R. Fett, 1989: An ice breeze mechanism for boundary-layer Jets. *Bound.-Layer Meteor.,* **48**, 177–195.

Moritz, R. E., 1977: On a possible sea-breeze circulation near Barrow, Alaska. *Arctic and Alpine Research,* **9**, 427–431.

National Ice Center, cited 2016: Current Daily Ice Products. http://www.natice.noaa.gov/Main_Products.htm

Navy, U.S., 2014: U.S. Navy arctic roadmap 2014–2030. Navy Task Force Climate Change 43pp, [Available online at: http://www.navy.mil/docs/USN_arctic_roadmap.pdf]

Persson, P. O. G., and T. Vihma, 2016: The atmosphere over sea ice. Chapter 6, *Introduction to Sea Ice,* 3rd Edition. Edited by David N. Thomas, Wiley-Blackwell, London. In press.

Reiter, E. R., 1963: The structure of jet streams. *Jet-Stream Meteorology.* The University of Chicago Press, 117–274.

ReVelle, D., and E. Nilsson, 2007: Summertime Low-Level Jets over the High-Latitude Arctic Ocean. *J. Appl. Meteor. Climatol.,* **47**, 1770–1784, doi:10.1175/2007JAMC1637.1

Shapiro, A., E. Fedorovich, 2010: Analytical description of a nocturnal low-level jet. *Q. J. R. Meteorol. Soc.,* **136**, 1255–1262, doi:10.1002/qj.628

Stull, R. B., 1988: *An Introduction to Boundary Layer Meteorology*, Springer, 670 pp., 1988.

Stull, R. B., 2009 Micrometeorology, Eos Trans. *AGU*, **90**, 7, doi: 10.1029/2009/2009EO010010

Tuononen, M., V. Sinclair, and T. Vihma, 2015: climatology of low-level jets in the mid-latitudes and polar regions of the Northern Hemisphere. *Atmos. Sci. Let.,* **16**, 492–499, doi:10.1002/asl.587

Vaisala, 2013: Viasala Radiosonde RS92-SGP. Accessed 02 November 2016. [Available online at http://www.vaisala.com/Vaisala%20Documents/Brochures %20and%20Datasheets/RS92SGP-Datasheet-B210358EN-F-LOW.pdf]

# INITIAL DISTRIBUTION LIST

1. Defense Technical Information Center
   Ft. Belvoir, Virginia

2. Dudley Knox Library
   Naval Postgraduate School
   Monterey, California